Producing the Dutch and Belgian mortality projections: a stochastic multi-population standard

Antonio, K.; Devriendt, S.; de Boer, W.; de Vries, R.; De Waegenaere, A.; Kan, H.-K.; Kromme, E.; Ouburg, W.; Schulteis, T.; Slagter, E.; van der Winden, M.; van Iersel, C.; Vellekoop, M.

DOI
10.1007/s13385-017-0159-x

Publication date
2017

Document Version
Final published version

Published in
European Actuarial Journal

Eur. Actuar. J. (2017) 7:297–336
https://doi.org/10.1007/s13385-017-0159-x

ORIGINAL RESEARCH PAPER

Producing the Dutch and Belgian mortality projections: a stochastic multi-population standard

Katrien Antonio[1,2,5] · Sander Devriendt[1] · Wouter de Boer[4] · Robert de Vries[4] · Anja De Waegenaere[3,5] · Hok-Kwan Kan[5,6] · Egbert Kromme[4,10] · Wilbert Ouburg[2,5,7] · Tim Schulteis[4,8] · Erica Slagter[5,6] · Marco van der Winden[4,9] · Corné van Iersel[4] · Michel Vellekoop[2,4]

Received: 10 February 2017 / Revised: 30 June 2017 / Accepted: 18 August 2017 /
Published online: 14 October 2017

Abstract The quantification of longevity risk in a systematic way requires statistically sound forecasts of mortality rates and their corresponding uncertainty. Actuarial associations have a long history and continue to play an important role in the development, application and dispersion of mortality projections for the countries they represent. This paper gives an in depth presentation and discussion of the mortality projections as published by the Dutch (in 2014) and Belgian (in 2015) actuarial associations. The goal of these institutions was to publish a stochastic mortality projection model in line with both rigorous standards of state-of-the-art academic work as well as the requirements of practical work such as robustness and transparency. Constructed by a team of authors from both academia and practice, the developed mortality projection standard is a Li and Lee type multi-population

Hok-Kwan Kan, Egbert Kromme, Wilbert Ouburg, Tim Schulteis, Erica Slagter, Marco van der Winden: This paper reflects the personal views of the author and not the views of his or her company.

✉ Sander Devriendt
sander.devriendt@kuleuven.be

[1] Faculty of Economics and Business, KU Leuven, Belgium

[2] Faculty of Economics and Business, University of Amsterdam, Amsterdam, The Netherlands

[3] Center for Economic Research (CentER), Tilburg University, Tilburg, The Netherlands

[4] Commissie Sterfte Onderzoek, Koninklijk Actuarieel Genootschap, Utrecht, The Netherlands

[5] Werkgroep Prognosetafels, Koninklijk Actuarieel Genootschap, Utrecht, The Netherlands

[6] Aegon, The Hague, The Netherlands

[7] Delta Lloyd, Amsterdam, The Netherlands

[8] Algemene Pensioen Groep (APG), Heerlen, The Netherlands

[9] PGGM, Zeist, The Netherlands

[10] KPMG, Amstelveen, The Netherlands

model. To project mortality, a global Western European trend and a country-specific deviation from this trend are jointly modelled with a bivariate time series model. We motivate and document all choices made in the model specification, calibration and forecasting process as well as the model selection strategy. We show the model fit and mortality projections and illustrate the use of the model in several pension-related applications.

Keywords Stochastic mortality models · Projected mortality · Stochastic multi-population mortality · Li and Lee model · Lee and Carter model · Poisson regression · Pension calculations · Longevity risk · Professional actuarial associations

1 Introduction

Life insurers, pension funds, health care providers and social security institutions work every day with life contingent liabilities, that is cash flows depending on a beneficiary being alive or not. This myriad of institutions faces increasing expenses due to continuing improvements of mortality rates, as discussed in Albrecher et al. [1]. Underestimating future mortality improvements implies a risk since it may lead to incorrect premium, provision and pension cost calculations. The International Monetary Fund (IMF) already affirmed the importance of this longevity risk in IMF [31],[1] and the European Commission recently examined the possible consequences in European Commission (DG ECFIN) and Economic Policy Committee (Ageing Working Group) [27].[2] The Commission estimates that in 2060 57.6% of the public pensioners in the European Union will be aged 75 or older whereas in 2013 this was only 36%.[3] To anticipate these growing ageing costs, various governments have made important adaptations to their pension systems and legislation. For example, pension reforms in The Netherlands impose that, from 2022 on, the official yearly retirement age increase is linked directly to the evolution of the period life expectancy of a 65-year old.[4] In Belgium, the official retirement age will increase to 67 in 2030.[5] The Belgian 'Commissie Pensioenhervorming 2020–2040', a group of academics in charge of proposing and preparing durable pension reforms, also suggests various changes to current pension policies[6] and proposes a mechanism to link career length to period life expectancy in order to ensure sustainable pension costs in the future.

[1] We refer to *Chapter 4. The financial impact of longevity risk.*

[2] We refer to *Part II: Long-term projections of age-related expenditure and unemployment benefits.*

[3] See Table II.1.15 in European Commission (DG ECFIN) and Economic Policy Committee (Ageing Working Group) [27], p. 79.

[4] See, for example, the 'Algemene Ouderdomswet' (AOW-law): http://wetten.overheid.nl/BWBR0002221/. The definition of period life expectancy is given in Sect. 5.1.

[5] The specific law was published on 21 August 2015, see http://reflex.raadvst-consetat.be/reflex/pdf/Mbbs/2015/08/21/131341.pdf.

[6] See, for example, their 2014 and 2015 reports: Commissie Pensioenhervorming 2020–2040 [14, 15].

The quantification of longevity risk in a systematic way requires sound forecasts of mortality rates and their corresponding uncertainty, as Barrieu et al. [4] indicate. Actuarial institutions have a long history and continue to play an important and active role in the development, application and dispersion of mortality tables and models, at the level of both population and insured portfolio data. For example, the 'Continuous Mortality Investigation Committee' (CMI) of the 'Institute and Faculty of Actuaries' (IFA) in the UK has been researching mortality of insured lives, based on data of associated insurance companies, and publishes mortality tables since 1924.[7] The 'Society of Actuaries' (SOA) also developed numerous mortality tables for reserving and valuation purposes which are endorsed by the 'National Association of Insurance Commissioners'[8] and imposed by many state insurance regulators in the USA. The Dutch 'Koninklijk Actuarieel Genootschap' (KAG) has a rich history in providing (with regular updates) nation-wide period mortality tables starting from the 1970's. Since 2007, KAG also publishes mortality projections which are currently updated biennially. The KAG 2012 mortality projection[9] uses Dutch smoothed mortality data to project mortality via a combination of a short and a long term trend model. Both IFA and SOA developed mortality projection models[10] based on smoothed historical mortality improvement rates of England and Wales and the US respectively. Subsequently, projections follow by using extrapolation methods combined with smoothing techniques, such that eventually a steady improvement rate results. The aforementioned approaches share some characteristics. The KAG 2012, IFA 2012 and SOA 2014 methods all start from country-specific historical data, transformed and smoothed, upon which a deterministic projection technique is then applied. This approach has its limitations in light of risk management with life contingent liabilities since it relies on extrapolation rather than statistical modelling techniques and only delivers a single scenario for future mortality rates. Hence, quantification of the uncertainty that comes with this projection is not possible.

This paper describes the set-up and technical specifications of the mortality projections published by KAG in 2014 and IA|BE in 2015, which implied major methodological changes compared to earlier projections by these institutions. Developed under the guidance of academic researchers, this mortality model is widely disseminated in practice for premium, reserve and general risk management calculations. During the development process the preference for a *stochastic* approach became clear, since a scenario generator allows to take uncertainty in forecasts into account and is therefore necessary in managing life contingent risks. This emphasis on stochastic mortality projection models receives wide coverage in the state-of-the-art actuarial, demographic and statistical literature, starting from the seminal work by Lee and Carter (LC) (see [38]). Moreover, a *multi-population* projecting model is recommended since it allows to enrich the country-specific data

[7] More history on the CMI can be found in Institute of Actuaries and Faculty of Actuaries [33], pp. 1–5.

[8] For example, the 2012 IAM and IAR, GAM–83 and GAR–94, see National Association of Insurance Commissioners [41], section 3.

[9] A complete description of the model is in Koninklijk Actuarieel Genootschap [36].

[10] We refer to Institute and Faculty of Actuaries [32] and Society of Actuaries [48] for more information.

with observations from countries with similar characteristics. At the same time differences in mortality rates between such countries are likely to stabilize over time, motivating the need for non-diverging multi-population projections. To accommodate the aforementioned needs, the KAG 2014 (see [37]) and IA|BE 2015 (see [3]) mortality projection models are fully stochastic projection models of Li and Lee (LL) type, see Li and Lee [40]. A Lee and Carter model is imposed for the European mortality trend as well as for the country-specific deviation from this common trend. KAG in 2014 and IA|BE in 2015 preferred this LL model based on a comparative analysis of stochastic projection models proposed in recent scientific literature. As part of this comparative exercise KAG and IA|BE studied the single population mortality models, fitted on country-specific data, from the papers by Cairns et al. [9], Haberman and Renshaw [29], Börger et al. [5] and Van Berkum et al. [50], the multi-population mortality models of Li and Lee [40] as well as additional multi-population models constructed in a similar way as recently proposed in Haberman et al. [28].[11] This collection of mortality models was evaluated using the criteria proposed in Cairns et al. [9], supplemented with the institutions' own points of attention regarding biological reasonableness, robustness, statistical performance and transparency.

Other tracks in current research on multi-population mortality models include the country-specific Lee Carter model in D'Amato et al. [17, 18] where the focus is on inter-population dependency, modeled using a VAR panel sieve approach, the common age effect specification of Kleinow [35], the copula approach in Chen et al. [13], and the recent functional data method in Shang [47]. D'Amato et al. [17], Chen et al. [13] and Shang [47] do not use a Poisson assumption on the number of deaths and therefore do not explicitly take into account the noise in the data. Moreover, the focus of these papers, as well as D'Amato et al. [18], is on in-sample accuracy and not (or only marginally) on the performance of the forecasts which was the main performance measure for our model.

Initially developed as a mortality forecasting method for The Netherlands, the model is easily applied to other European countries. We explain the methodology with a focus on the Dutch and Belgian case, but provide some graphical results for France and West-Germany in the Appendix. The French and German results are purely illustrative as we did not include up-to-date data nor went through the complete model evaluation process for these countries. This paper provides a full documentation, discussion and validation of the preferred model and points out the key choices and assumptions involved in the selection process of creating an industry wide standard for mortality projections. We illustrate typical use of the scenarios generated by the model in the measurement and management of life contingent risks. Moreover, as existing literature does not typically elaborate on the data treatment, we carefully explain how mortality statistics collected from different sources, each with its own pace of refreshing the data, can be combined.

This paper is organized as follows. The source and extent of the available data as well as the data manipulations are explained in Sect. 2. A technical description of

[11] The multi-population models in this report consist of various combinations of mortality models for the multi-population trend and the country-specific deviation.

the model is in Sect. 3. The fitting and projecting results of this model are documented in Sect. 4. Section 5 presents four applications which demonstrate the relevance of the stochastic mortality model on policy making and life contingent calculations. Section 6 concludes. Full parameter estimates and the resulting KAG 2014 and IA|BE 2015 mortality projection for The Netherlands and Belgium are available online.[12]

2 Data

2.1 Notation

Let $\mathcal{X}$ denote a collection of integer ages and $\mathcal{T}$ a collection of integer years. We denote with $q_{x,t}$ the probability that a person who is alive at 1 January of year t, and who was born on 1 January of year $t-x$, will not be alive on 1 January of year $t+1$, for $x \in \mathcal{X}$ and $t \in \mathcal{T}$. We call $q_{x,t}$ the mortality rate at exact age x in year t. The stochastic mortality models discussed in the papers mentioned in Sect. 1 model (a transformation of) $q_{x,t}$ or the force of mortality, $\mu_{x,t}$. We assume a piecewise constant force of mortality, i.e. $\mu_{x+s,t+s} = \mu_{x,t}$ for $0 \leq s < 1$. The following relation then holds between $q_{x,t}$ and $\mu_{x,t}$:

$$q_{x,t} = 1 - \exp(-\mu_{x,t}). \tag{1}$$

Expression (1) enables switching from the force of mortality to the mortality rate, and vice versa, in a straightforward way. For more details about these concepts and additional reading material we refer to Pitacco et al. [43].

We denote by $d_{x,t}$ the total death count of people aged x who die in year t before they reach age $x+1$. The total amount of *person years* lived by people aged $[x, x+1)$ in year $[t, t+1)$ is called the 'exposure to risk', denoted by $E_{x,t}$. The central death rate $m_{x,t}$ is then

$$m_{x,t} = \frac{d_{x,t}}{E_{x,t}}. \tag{2}$$

Under the assumption of piecewise constant force of mortality, the maximum likelihood estimate $\hat{\mu}_{x,t}$ of the force of mortality is given by

$$\hat{\mu}_{x,t} = m_{x,t}. \tag{3}$$

All the aforementioned quantities are referred to as being in 'exact age' or 'period age'. They apply to people who have exact age x at exact time t. We illustrate the concepts of deaths and exposures in the left Lexis diagram in Fig. 1. The straight lines represent individuals' life lines as they age through time. For example, life line z (left graph) stops in year t at an age between x and $x+1$ and will thus be counted in $d_{x,t}$. The person has survived in year t for slightly less than half a year and this

[12] For the Belgian calibration, see http://www.iabe.be/nl/iabe-mortality-tables. For the Dutch calibration, see http://www.ag-ai.nl/view.php?action=view&Pagina_Id=480.

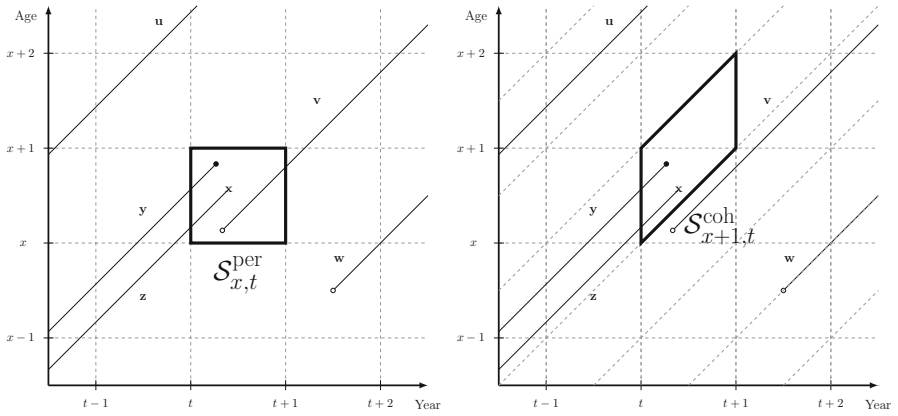

Fig. 1 Lexis diagram with life lines `u, v, w, y, z` and representation of period (left) and cohort (right) surfaces. `x` marks the death of a person, • indicates a person dropping out of the study alive, ○ specifies a new person entering the study. In our study, only birth and death are observed

fraction contributes to the exposure $E_{x,t}$. The death count $d_{x,t}$ and exposure $E_{x,t}$ are therefore measured over all life lines passing through the square surface $\mathcal{S}^{\text{per}}_{x,t}$ in Fig. 1 (left). Denote with (a, b) a person with exact age a at exact time b. The surface $\mathcal{S}^{\text{per}}_{x,t}$ is then represented in the following way:

$$\mathcal{S}^{\text{per}}_{x,t} = \{(a,b) \mid x \le a < x+1;\ t \le b < t+1\}. \tag{4}$$

As Cairns et al. [10] indicate, one has to be wary of any data quality issues when receiving data from different sources or even from the same source at different times. For example, not all data sources work with these period or exact age definitions of deaths and exposure, but instead apply 'cohort' or 'completed years' definitions.[13] A cohort refers to all people born in the same year. On 1 January of year t, a cohort born in year $t-x-1$ will have 'completed' the exact age x and not reached age $x+1$. The probability that a person with completed age x at 1 January of year t dies within 1 year, is called the cohort death rate or mortality rate. The associated cohort number of deaths, $d^{\text{coh}}_{x+1,t}$,[14] is the number of people born in the year $t-x-1$ who died in year t. A similar definition applies to the cohort exposures $E^{\text{coh}}_{x+1,t}$. As the life lines move diagonally through a Lexis diagram, the surface $\mathcal{S}^{\text{coh}}_{x+1,t}$ in which the cohort quantities are measured has the shape of a parallelogram, as illustrated in Fig. 1 (right). A person who is represented by the age-time pair (a, b) was born at exact time $c = b - a$. The time of birth c allows for an easy representation of the cohort surface $\mathcal{S}^{\text{coh}}_{x+1,t}$:

[13] For example, these definitions are used by 'Centraal Bureau voor Statistiek' (CBS, http://www.cbs.nl/en-GB/menu/home/default.htm?Languageswitch=on) in The Netherlands and 'Algemene Directie Statistiek—Statistics Belgium' (ADS, http://statbel.fgov.be/en/statistics/figures/) in Belgium.

[14] We use the CBS definitions where the age-time subscript 'x, t' refers to people born in year $t-x$. Other institutions, such as the ADS, use 'x, t' to refer to people born in year $t-x-1$.

$$\mathcal{S}^{\text{coh}}_{x+1,t} = \{(a,b) \mid t-x-1 \leq c < t-x;\ t \leq b < t+1;\ c = b-a\}. \tag{5}$$

As some institutions publish data on deaths and exposures only in the cohort representation while others use the exact age definitions, it will be necessary to establish a link between the cohort and period deaths and exposures. Such a link enables to transform data displayed in the format of the left panel in Fig. 1 to the format of the right panel, and vice versa. We refer to Sect. 2.3 for the details.

2.2 European data from human mortality database

We construct our multi-population mortality model using data from a pool of European countries with similar socio-economic characteristics, available from the human mortality database[15] (HMD). According to Niu and Melenberg [42] a positive dependence exists between mortality rates and gross domestic product (GDP) per capita. Therefore our approach calibrates the multi-population mortality model using the European countries with GDP per capita above the Eurozone average.[16] This leads to a pool of 14 countries (from largest exposure to smallest): West-Germany, France, England and Wales, The Netherlands, Belgium, Sweden, Austria, Switzerland, Denmark, Finland, Norway, Ireland, Luxembourg and Iceland. East-Germany, Scotland and Northern Ireland are not included since they were less economically developed during part of the calibration period (see further) or because HMD mentioned quality issues with the data. As such we create a multi-country dataset with a composition as illustrated in Fig. 2. Figure 3 shows the observed evolution of the period life expectancy at birth, see Sect. 5.1, in the aforementioned countries over time. The life expectancy of these countries has been slowly converging since 1970.

From the HMD database we use the tables 'Deaths' and 'Exposure to risk' in 1×1 format for the countries listed above. HMD provides these quantities following the *exact age* definitions[17] which correspond to the square region in Fig. 1 (left). We use an age range $\mathcal{X} = \{0, \ldots, 90\}$ and a period range $\mathcal{T} = \{1970, \ldots, 2009\}$. To enable a proper calibration of the stochastic model proposed in Sect. 3.1 on old age statistics, the age range is capped at 90 because the data for ages above 90 has not enough exposure and volatile data result. A calibrated parametric law will extrapolate the calibrated force of mortality towards higher ages, also known as 'closing the life table'. Our strategy to close the resulting mortality forecasts for old ages is described in Sect. 3.3. The start of the calibration period is motivated by the increasing convergence in life expectancy between the relevant countries since 1970, as illustrated in Fig. 3. Moreover, the chosen period is long enough to allow a stable calibration. For a univariate Lee–Carter (LC) calibration of Dutch and Belgian mortality data, a starting year around 1970 has

[15] This mortality database is available at http://www.mortality.org.

[16] Source: World Bank Data for 2013 on GDP per capita in US dollar, http://data.worldbank.org/indicator/NY.GDP.PCAP.CD.

[17] See bottom of page 6 in the HMD protocol: http://www.mortality.org/Public/Docs/MethodsProtocol.pdf.

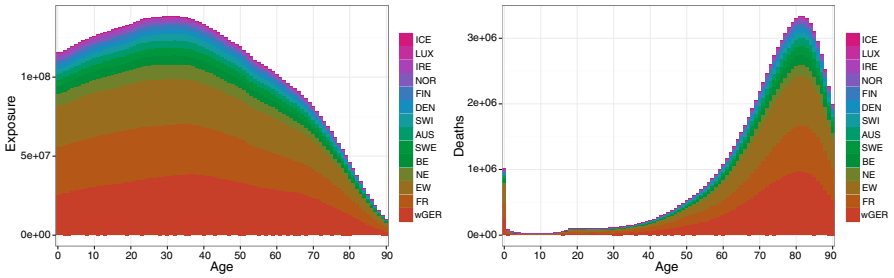

Fig. 2 Combined female and male exposures (left) and deaths (right) for all ages and stacked per country. The countries are sorted and the country with the highest exposure and deaths is at the bottom of the graph

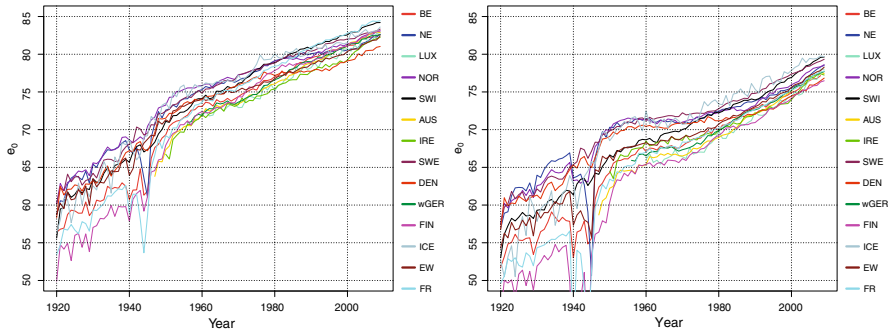

Fig. 3 Evolution from 1920 to 2009 of the period life expectancy for a newborn, female (left) and male (right). Data is the period 'Life expectancy at birth' from HMD (file E0per.txt)

been suggested as a structural break for Dutch males in Van Berkum et al. [50] or as the start of an optimal calibration period in Denuit and Goderniaux [21]. The last year for which mortality data is available from HMD for all countries under consideration was 2009.[18]

2.3 Official country-specific data: the case of The Netherlands and Belgium

To design a multi-population mortality projection model we combine the most recent data of the country of interest with a larger data set downloaded from the HMD. The large multi-country data base (from HMD) is typically refreshed with significant delay compared to the data published by the official statistics institution of a single country. We sketch the necessary transformations to go from data in *completed years* format (which country-specific institutions may use) to *exact age* format (which HMD uses), and vice versa. We illustrate these transformations for The Netherlands. Similar transformations will be necessary when combining HMD data with more recent data for other countries.

[18] Since we reproduce the results and forecasts as published by KAG on 9 September 2014 and by IA|BE on 18 February 2015 we use the data used by the authors of these publications, as downloaded on 29 May 2014.

At the time of analysis, the most recent calendar year of data available on HMD was 2009 for The Netherlands and 2012 for Belgium.[19] In order to be able to work with the most recent data, Dutch deaths ($d_{x,t}^{(\mathrm{NE})}$) and exposures ($E_{x,t}^{(\mathrm{NE})}$), for $t \in \{2010, 2011, 2012, 2013\}$ were obtained from CBS statistics. Similarly, Belgian deaths and exposures were procured via ADS statistics. Both institutions provide the information only in *completed years* which requires a transformation to the *exact age* definition, in order to merge the institutional data with the HMD data from Sect. 2.2.

As illustrated in Fig. 1, the cohort, or completed age, definition counts the number of deaths and exposures in a parallelogram instead of a square. To transform cohort data into period, or exact age, data, we follow the HMD protocol.[20] Consider the Dutch case and denote the CBS cohort death counts[21] with $d_{x+1,t}^{(\mathrm{CBS})}$, and the HMD period death counts with $d_{x,t}^{(\mathrm{NE})}$. These quantities have the same starting point (x, t) in the Lexis age-time diagram, as illustrated by the bullet (•) in Fig. 4. We divide the parallelogram and the square, over which the deaths are counted, into triangles as visualized in Fig. 4. The upper triangle from the period death count then corresponds to the lower triangle of the cohort death count. In line with the HMD protocol, the death counts $d_{x,t}^{(\mathrm{CBS})}$ and $d_{x,t}^{(\mathrm{NE})}$ are assumed to be spread uniformly over the surfaces. By rearranging the triangles, the cohort death counts are then transformed into period death counts as follows:

$$d_{x,t}^{(\mathrm{NE})} = \frac{1}{2} d_{x,t}^{(\mathrm{CBS})} + \frac{1}{2} d_{x+1,t}^{(\mathrm{CBS})} \quad \text{if } x > 0 \tag{6}$$

$$d_{0,t}^{(\mathrm{NE})} = d_{0,t}^{(\mathrm{CBS})} + \frac{1}{2} d_{1,t}^{(\mathrm{CBS})}, \tag{7}$$

where $d_{0,t}^{(\mathrm{CBS})}$ is the death count of people born in year t who died before 1 January of year $t + 1$.

To combine data from the parallelogram display with data in the square display we also need to calculate the exposure over the square region in Fig. 5. CBS provides data on the population $p_{x,t}$ per age x at 1 January of year t and the deaths in the upper and lower triangle of the square, denoted by $d_{x,t}^{(U)}$ and $d_{x,t}^{(L)}$ in Fig. 4. Let $N_{x+1,t}$ be the number of people who attain age $x + 1$ during year t. Ignoring emigration and immigration,[22] the following formula holds:

[19] On 30 December 2015, data until 2012 for both The Netherlands and Belgium was available on HMD. This data was used to stay as close as possible to the original dataset used by KAG and IA|BE.

[20] This protocol is available from http://www.mortality.org/Public/Docs/MethodsProtocol.pdf.

[21] The number of deaths per year, age and gender are available at http://alturl.com/dz7mc.

[22] Data from, for example, CBS shows that the yearly net migration in recent years is around 0.2% of the total population and for specific ages is almost always less than 2%. We consider these effects small enough to not have a significant impact on the calculations. Population data from http://statline.cbs.nl/Statweb/publication/?DM=SLNL&PA=7461BEV&D1=0&D2=1-2&D3=1-100&D4=45-66&HDR=G1,G3,T&STB=G2&VW=T and migration data from http://statline.cbs.nl/Statweb/publication/?DM=SLNL&PA=03742&D1=3&D2=1-2&D3=1-96&D4=0&D5=0&D6=a&HDR=G3,T,G1,G5&STB=G4,G2&VW=T.

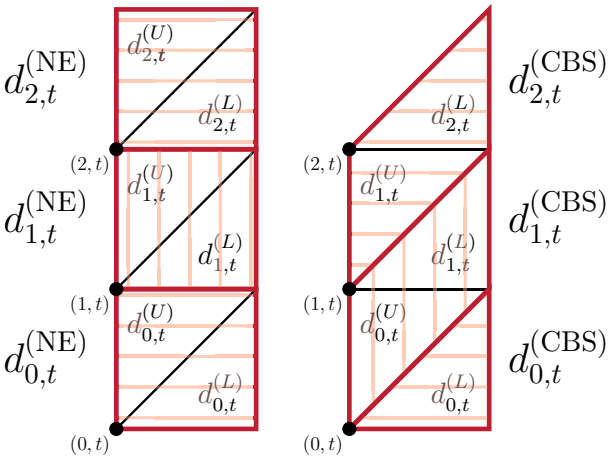

Fig. 4 Comparison between one year period (left) and cohort (right) death counts starting with all people aged [0, 3) at exact time t

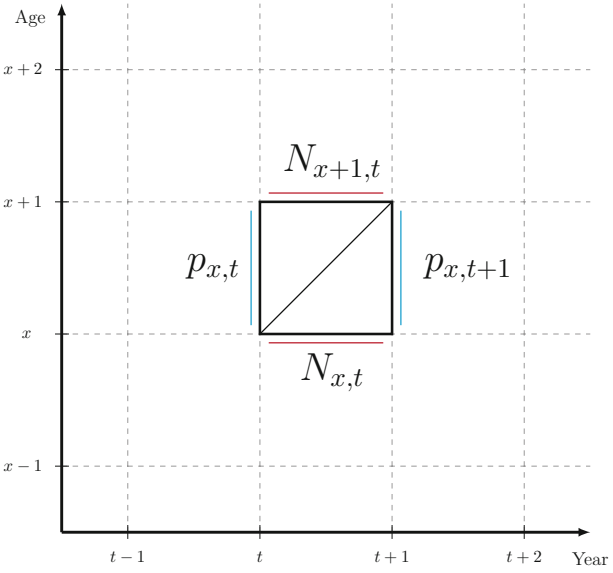

Fig. 5 Graphical representation of population metrics in the Lexis diagram. The population size of the cohort aged $[x, x+1)$ on 1 January of year t is represented by $p_{x,t}$ and the population reaching exact age x at year $[t, t+1)$ is $N_{x,t}$

$$N_{x+1,t} = p_{x,t} - d^{(U)}_{x,t}. \tag{8}$$

Assuming that the birthdays of people reaching age $x+1$ in year t are distributed uniformly over the year, the average amount of time a person from the group of

$N_{x+1,t}$ people spends in the upper triangle $d_{x,t}^{(U)}$ is half a year. The contribution of people aged x reaching their next birthday in year t to the exposure in the upper triangle ($E_{x,t}^{(U)}$) is then $\frac{1}{2}N_{x+1,t}$. The contribution to the exposure $E_{x,t}^{(U)}$ of the people not surviving until their next birthday can be derived using a geometrical argument. Because of the assumption of a uniform distribution of deaths over the triangles, the barycenter of the deaths within the upper triangle is the age-time point $(x+\frac{2}{3}, t+\frac{1}{3})$. Thus, someone who dies in the upper triangle $d_{x,t}^{(U)}$ contributes $\frac{1}{3}$ years on average to the exposure in the upper triangle $E_{x,t}^{(U)}$. Adding the exposure of the deceased to the exposure of the people surviving the upper triangle, we obtain the following formula for the exposure within the upper triangle:

$$E_{x,t}^{(U)} = \frac{1}{2}N_{x+1,t} + \frac{1}{3}d_{x,t}^{(U)} \tag{9}$$

$$\overset{(8)}{=} \frac{1}{2}p_{x,t} - \frac{1}{6}d_{x,t}^{(U)} \tag{10}$$

$$\overset{(6)}{=} \frac{1}{2}p_{x,t} - \frac{1}{6}\left(\frac{1}{2}d_{x+1,t}^{(\mathsf{CBS})}\right) \quad \text{if } x > 0 \tag{11}$$

$$E_{0,t}^{(U)} \overset{(7)}{=} \frac{1}{2}p_{0,t} - \frac{1}{6}d_{1,t}^{(\mathsf{CBS})} \ . \tag{12}$$

Similar arguments hold for the exposure in the lower triangle $E_{x,t}^{L}$. Recombining the triangle exposures into square period exposures leads to the following formulas:

$$E_{x,t}^{(\mathrm{NE})} = E_{x,t}^{(U)} + E_{x,t}^{(L)} \tag{13}$$

$$\overset{(11)}{=} \frac{1}{2}\left(p_{x,t} + p_{x,t+1}\right) + \frac{1}{12}\left(d_{x,t}^{(\mathsf{CBS})} - d_{x+1,t}^{(\mathsf{CBS})}\right) \quad \text{if } x > 0 \tag{14}$$

$$E_{0,t}^{(\mathrm{NE})} \overset{(12)}{=} \frac{1}{2}\left(p_{0,t} + p_{0,t+1}\right) + \frac{1}{6}\left(d_{0,t}^{(\mathsf{CBS})} - \frac{1}{2}d_{1,t}^{(\mathsf{CBS})}\right). \tag{15}$$

For the case of Belgium, ADS uses the same cohort definition as CBS but with a slightly different notation. This implies minor changes to the above formula's. See Antonio et al. [3] for more details.

3 Model set-up, calibration and projection

This section presents the model set-up, calibration and projection strategy of our stochastic multi-population model. It should be emphasized that the goal of the Dutch and Belgian institutions was the development of an industry standard for country-specific projections of mortality, relevant for life contingent calculations. More specifically, it was required to build a stochastic mortality projection model on

the complete age range (starting from age 0, running up to age 120) in line with both the rigorous standards of state-of-the-art academic work (see [9]) as well as the requirements of practical work such as robustness, biological reasonableness, interpretability and transparency.

The use of a stochastic model integrating data from multiple populations was key in the model selection process, as motivated in Sect. 1. Additionally, statistical performance of a wide range of mortality models was evaluated with the Bayesian Information Criterion (BIC, see [46]) and proper scoring rules for count data, see Czado et al. [16].[23] As such, the model from Li and Lee [40] performed very well on this set of criteria and outperformed the models listed in Cairns et al. [9], Haberman and Renshaw [29], Börger et al. [5], Van Berkum et al. [50] and Haberman et al. [28] which were also part of the comparative study. Haberman et al. [28] and Cairns and El Boukfaoui [11] did not prefer the LL model in their study of basis risk because—for certain ages—near-perfect correlation may be present between the reference population and the smaller book population. This may indeed create problems when assessing basis risk, where projections should reflect possibly different evolutions in the mortality trend of a reference population and a book of insureds. The goal in our case is not to assess basis risk, but to assess the quality of country-specific mortality projections. Hence, other criteria such as robustness and biological reasonableness were deemed more important. For example, in models with cohort effects, the cohort turned out to be hard to estimate and project in a robust way, with similar problems as indicated in Plat [44] and Renshaw and Haberman [45]. Thus, eventually, the group of academics and practitioners behind Koninklijk Actuarieel Genootschap [37] and Antonio et al. [3] selected the model specification of Li and Lee [40] to develop their industry standard. Full details are given in this section.

3.1 Model set-up

The force of mortality of the country under consideration is denoted by $\mu_{x,t}^{(c)}$, the European force of mortality by $\mu_{x,t}^{(\mathrm{EU})}$, and the country's deviation from the European force of mortality by $\widetilde{\mu}_{x,t}^{(c)}$. In the case of KAG or IA|BE, $c \in \{\mathrm{NE}, \mathrm{BE}\}$ refers to The Netherlands and Belgium respectively. We emphasize that the model is fitted separately for Dutch and Belgian data. In line with the goals of the national actuarial associations, the model, as presented in this paper, is designed to project and evaluate the mortality of one country at a time as it does not jointly model the deviations of all individual countries together. The Li and Lee (LL) mortality model specifies the logarithm of the force of mortality for the country under consideration, $\mu_{x,t}^{(c)}$, as follows

[23] Proper scoring rules are out-of-sample evaluation criteria. They are used to assess model predictions by allocating a score for each prediction, based on its accuracy and sharpness. Examples of these scores are the predictive deviance, the squared Pearson residuals or the Dawid–Sebastiani scoring rule from Dawid and Sebastiani [19].

$$\ln \mu_{x,t}^{(c)} = \ln \mu_{x,t}^{(\mathrm{EU})} + \ln \widetilde{\mu}_{x,t}^{(c)} \tag{16}$$

$$\ln \mu_{x,t}^{(\mathrm{EU})} = A_x + B_x K_t \tag{17}$$

$$\ln \widetilde{\mu}_{x,t}^{(c)} = \alpha_x^{(c)} + \beta_x^{(c)} \kappa_t^{(c)}. \tag{18}$$

We recognize two times a Lee and Carter specification; Eq. (17) is a LC model for the European evolution of mortality (driven by $\mu_{x,t}^{(\mathrm{EU})}$) and (18) is a LC model for the country-specific deviation from this common trend (specified by $\widetilde{\mu}_{x,t}^{(c)}$). All parameters with superscript (c) are country-specific and will therefore change when fitting the model for a different country under consideration. We discuss the methodology used to calibrate the parameters in (17) and (18) in Sect. 3.2. In order to project the fitted force of mortality into the future, we approach the fitted time dependent effects (K_t and $\kappa_t^{(c)}$) as realizations of a bivariate time series. This choice of time series and projection strategy is documented and motivated in Sect. 3.3. We project the time series, K_t and $\kappa_t^{(c)}$, using the following specification:

$$K_{t+1} = K_t + \theta^{(c)} + \epsilon_{t+1}^{(c)} \tag{19}$$

$$\kappa_{t+1}^{(c)} = a^{(c)} \kappa_t^{(c)} + \delta_{t+1}^{(c)}. \tag{20}$$

The dynamics of the common period effect (see (19)), K_t, are modelled with a random walk with drift (RWD), where $\theta^{(c)}$ is the drift. The country-specific period effect (see (20)), $\kappa_t^{(c)}$, follows an AR(1) process without intercept, as in Li and Lee [40]. The error terms, $(\epsilon_{t+1}^{(c)}, \delta_{t+1}^{(c)})$, for the time series are possibly correlated Gaussian random variables with an independent and identical distribution over time. We calibrate the parameters in these time series specifications on the estimated K_t and $\kappa_t^{(c)}$ parameters for $t \in \mathcal{T}$, and use these dynamics to project $\mu_{x,t}^{(c)}$ for future t. Since the calibration methodology allows for possible correlation between the two time series, the parameters in (19) and (20) (including the drift $\theta^{(c)}$) change when a different country of interest is used. We further explain this in Sect. 3.3.

3.2 Calibration, goodness-of-fit and robustness

We calibrate the parameters (A_x, B_x, K_t, $\alpha_x^{(c)}$, $\beta_x^{(c)}$ and $\kappa_t^{(c)}$) in the LL specification using maximum likelihood estimation (MLE). Following the seminal paper by Brouhns et al. [6] we assume a Poisson distribution for the number of deaths random variable $D_{x,t}$, with mean $E_{x,t} \cdot \mu_{x,t}$ and $E_{x,t}$ the observed exposure to risk. To avoid identification problems in the LL model we use a conditional maximum likelihood approach as in Li [39]. We calibrate the common parameters (i.e. A_x, B_x and K_t) on aggregated European data in a first step, followed by the calibration of the country-specific parameters (i.e. $\alpha_x^{(c)}$, $\beta_x^{(c)}$ and $\kappa_t^{(c)}$) using country-specific data in a second step. We explain this process in more detail below.

1. We obtain observed deaths, $d_{x,t}^{(\mathrm{EU})}$, and corresponding exposures to risk, $E_{x,t}^{(\mathrm{EU})}$, to calibrate the European trend by aggregating deaths and exposures downloaded from HMD (see Sect. 2) over the 14 selected countries, using $\mathcal{X} = \{0, \ldots, 90\}$ and $\bar{\mathcal{T}} = \{1970, \ldots, t_{\max}^{(\mathrm{EU})}\}$ where $t_{\max}^{(\mathrm{EU})}$ is the most recent calendar year for which data is available for the whole set of countries. In our case $t_{\max}^{(\mathrm{EU})} = 2009$, as outlined in Sect. 2.2. We maximize the following Poisson likelihood

$$\max_{\{A_x, B_x, K_t\}} \prod_{x \in \mathcal{X}} \prod_{t \in \bar{\mathcal{T}}} (E_{x,t}^{(\mathrm{EU})} \mu_{x,t}^{(\mathrm{EU})})^{d_{x,t}^{(\mathrm{EU})}} \cdot \exp\left(-E_{x,t}^{(\mathrm{EU})} \mu_{x,t}^{(\mathrm{EU})}\right) / (d_{x,t}^{(\mathrm{EU})}!), \tag{21}$$

with $\mu_{x,t}^{(\mathrm{EU})} = \exp(A_x + B_x K_t)$. We apply the usual Lee and Carter parameter constraints to identify parameters in a unique way, namely

$$\sum_{t \in \bar{\mathcal{T}}} K_t = 0 \quad \text{and} \quad \sum_{x \in \mathcal{X}} B_x = 1. \tag{22}$$

These constraints are applied immediately after every update of both the K_t and the B_x in the iterative optimization procedure, in correspondence with the `LifeMetrics` code on which our calibration program is based (see [7]). We refer to Chapter 5 in Pitacco et al. [43] for the precise Newton–Raphson formulas in the updating scheme. This step only requires data aggregated at European level and will thus lead to the same results irrespective of the country of interest.

2. For the country of interest, denoted with superscript (c), we want to use the most recent set of data when calibrating the mortality model. Since not all countries update their data at the same pace, a discrepancy will arise between the most recent year of data available for the specific country and for every other country in the set. Therefore, if data for the country of interest is available up to year $t_{\max}^{(c)}$, we need to extend the parameter estimates for K_t to the years $\{t_{\max}^{(\mathrm{EU})} + 1, \ldots, t_{\max}^{(c)}\}$. For this we use linear extrapolation which is justified by the linear trend observed in the K_t estimates (see top right corner of Fig. 6), namely

$$K_{t^{\mathrm{EU}}max+s} = K_{t^{(\mathrm{EU})}max} + s(K_{t^{(\mathrm{EU})}max} - K_{1970})/(t_{\max}^{(\mathrm{EU})} - 1970),$$

with $s \in \{1, \ldots, t_{\max}^{(c)} - t_{\max}^{(\mathrm{EU})}\}$. For The Netherlands and Belgium the data was, at the moment of publishing the IA|BE and KAG mortality prognoses, available from HMD up to 2012 and supplemented by data from national institutions up to $t_{\max}^{(c)} = 2013$.

3. We calibrate the country-specific parameters (i.e. $\alpha_x^{(c)}$, $\beta_x^{(c)}$ and $\kappa_t^{(c)}$) by maximizing the following Poisson likelihood, conditional on $\mu_{x,t}^{(\mathrm{EU})}$ as estimated in steps 1 and 2 of this procedure. Thus,

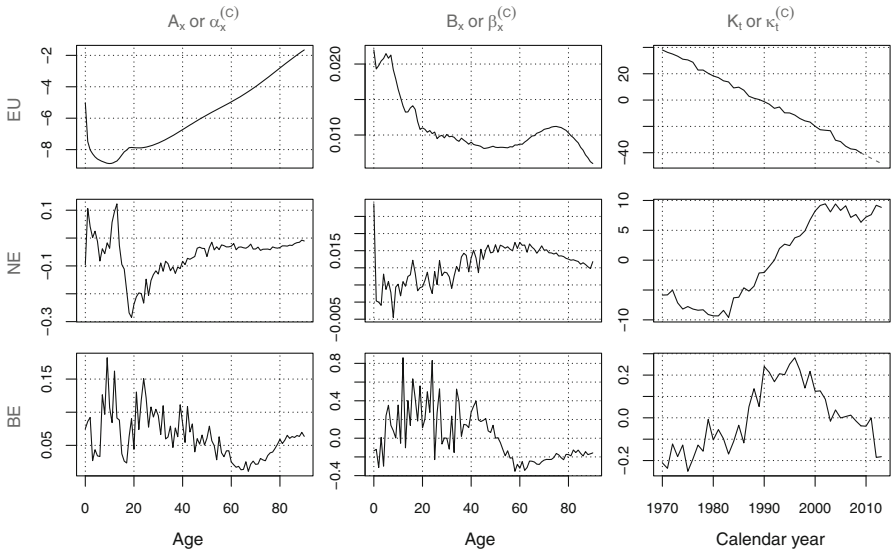

Fig. 6 Estimated parameters for the common trend (top row, A_x, B_x, K_t), Dutch deviation (middle row, $\alpha_x^{(\mathrm{NE})}$, $\beta_x^{(\mathrm{NE})}$ and $\kappa_t^{(\mathrm{NE})}$) and Belgian deviation (bottom row, $\alpha_x^{(\mathrm{BE})}$, $\beta_x^{(\mathrm{BE})}$ and $\kappa_t^{(\mathrm{BE})}$), female data, ages 0–90, years 1970–2013

$$\max_{\{\alpha_x^{(c)},\,\beta_x^{(c)},\,\kappa_t^{(c)}\}} \prod_{x\in\mathcal{X}}\prod_{t\in\mathcal{T}} (E_{x,t}^{(c)}\mu_{x,t}^{(c)})^{d_{x,t}^{(c)}} \cdot \exp\left(-E_{x,t}^{(c)}\mu_{x,t}^{(c)}\right)/(d_{x,t}^{(c)}!), \tag{23}$$

where $\mu_{x,t}^{(c)} = \mu_{x,t}^{(\mathrm{EU})} \cdot \exp\left(\alpha_x^{(c)} + \beta_x^{(c)}\kappa_t^{(c)}\right)$. We calibrate the country-specific parameters on ages $x \in \mathcal{X} = \{0,\ldots,90\}$ and years $t \in \mathcal{T} = \{1970,\ldots,t_{\max}^{(c)}\}$. Once again we normalize the estimated parameters after every iteration by imposing

$$\sum_{t\in\mathcal{T}} \kappa_t^{(c)} = 0 \quad \text{and} \quad \sum_{x\in\mathcal{X}} \beta_x^{(c)} = 1. \tag{24}$$

We apply this calibration strategy separately for male and female data as in Carter and Lee [12] and Brouhns et al. [6]. We illustrate the resulting parameter estimates for female data in Fig. 6 with the common parameters in the top, Dutch parameters in the middle and Belgian parameters in the bottom row.[24]

We illustrate the goodness-of-fit of our model with a heatmap of Pearson residuals[25] in Fig. 7. The model captures quite well the period and age effects where the residuals behave randomly. For cohorts, however, Fig. 7 exhibits an effect for Belgian and, slightly

[24] A complete set of all Dutch parameters can be found at the last pages of http://www.ag-ai.nl/download/20470-Prognosetafel+14-Appendix+A.pdf. The full set of Belgian parameters can be found at http://www.iabe.be/sites/default/files/bijlagen/mortality_tables_iabe_2015_parameters.xls.

[25] The Pearson residuals for the Poisson regression in our model are defined as $\frac{d_{x,t}^{(c)} - E_{x,t}^{(c)}\hat{\mu}_{x,t}^{(c)}}{\sqrt{E_{x,t}^{(c)}\hat{\mu}_{x,t}^{(c)}}}$.

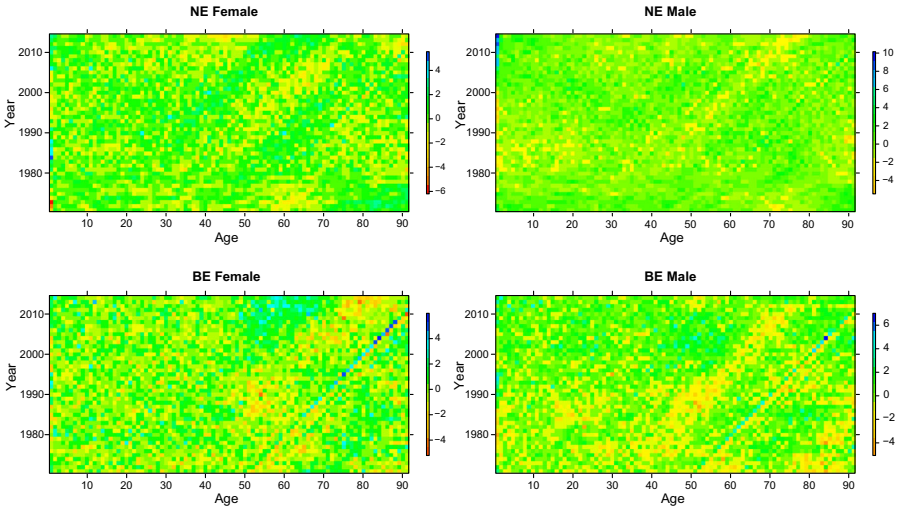

Fig. 7 Pearson residual heatmaps for the model fitted on Dutch (top row) and Belgian (bottom row), female (left column) and male (right column) data, ages 0–90, years 1970–2013

less pronounced, Dutch data. Our experiments with the inclusion of cohort effects in the model specification, revealed difficulties to find reasonable forecasts of these cohort effects, and problems with the robustness of the model. Van Berkum et al. [50] report similar problems for cohort effects in their study of different mortality models for The Netherlands and Belgium. We therefore opted not to include cohort effects in our model. Figure 8 shows the robustness of our model with respect to the calibration period used. All parameters exhibit the same behaviour and trend for the different calibration periods investigated, with a slight increase of parameter variability for Belgian data.

3.3 Projection

Calibrating the time series models The mortality model specified in Sect. 3.2 together with the time dynamics from (19) and (20) allow us to generate future scenarios of mortality and hence take uncertainty in these scenarios into account when performing life contingent calculations. The use of a RWD process for the common trend and an AR(1) process for the country-specific deviation enhances coherent forecasts in the sense that the mortality of the different countries will not diverge from the common trend, if the AR(1) process is stationary. For the country-specific deviation, any unstationary time series, such as RWD, will lead to divergence from the common trend and is therefore ruled out on biological grounds. The choice for the RWD and AR(1) processes and the concept of coherence is further motivated in Li and Lee [40] and Hyndman et al. [30].

First, we calibrate the time series models to the parameter estimates $\{(K_t, \kappa_t^{(c)}) \mid t \in \mathcal{T}\}$ with $\mathcal{T} = \{1970, \ldots, 2013\}$. We assume a bivariate normal distribution for the error terms $(\epsilon_t^{(c)}, \delta_t^{(c)})$ with mean $(0,\ 0)$ and covariance matrix $\boldsymbol{V}^{(c)}$. The error terms are

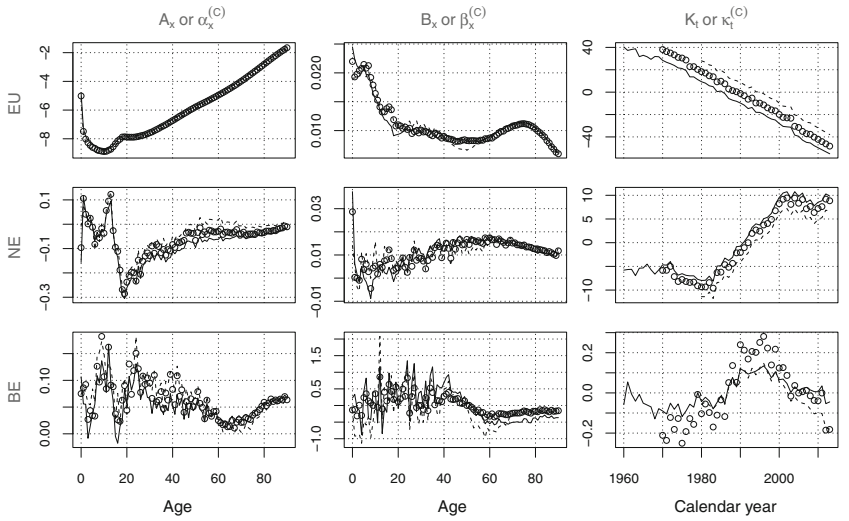

Fig. 8 Estimated parameters for the common trend (top row, A_x, B_x, K_t), Dutch deviation (middle row, $\alpha_x^{(\mathrm{NE})}$, $\beta_x^{(\mathrm{NE})}$ and $\kappa_t^{(\mathrm{NE})}$) and Belgian deviation (bottom row, $\alpha_x^{(\mathrm{BE})}$, $\beta_x^{(\mathrm{BE})}$ and $\kappa_t^{(\mathrm{BE})}$), female data, ages 0–90, for three calibration periods: parameters estimated on 1960–2013 data are denoted with a straight line (–), on 1970–2013 data with dots (○) and on 1980–2013 data with a dashed line (–). For the Belgian 1980–2013 calibration, β_x and κ_t have been rescaled by $-$ 12 and $-$ 1/12 respectively to enable a good comparison

independent and identically distributed for all t. The parameters $\theta^{(c)}$, $a^{(c)}$ and $\boldsymbol{V}^{(c)}$, used in the time series specifications, are estimated using maximum likelihood.[26] Since we incorporate correlation between the time series in the estimation procedure, the drift $\theta^{(c)}$ and the covariance matrix $\boldsymbol{V}^{(c)}$ will change if another country of interest is chosen. Modeling the multivariate time series of all country-specific deviations in the European data set simultaneously with the common trend, would be a way to overcome this feature. This approach is outside the scope of this paper. The resulting parameter estimates (for male and female data) follow in Table 1 for both the Dutch and Belgian calibration. For Dutch females and Belgian males the AR(1) parameter a is very close to, but strictly smaller than, one resulting in a stationary time series and coherent forecasts. Sect. 6 outlines several strategies, such as constrained optimization or Bayesian calibration, that can be used in case a calibration on different data leads to unstationary time series. In a case study with Austria, Belgium, Denmark, Sweden, Switzerland and Czechia, Enchev et al. [26] discuss the use of a RWD for country-specific period effects. Using this time series specification, they give up the requirement of coherence in multi-population forecasting, leading to divergent mortality rates of the different countries over time. Although $\theta^{(c)}$ represents the drift of the common trend K_t, it will change slightly when calibrating the model for a different

[26] In R we use Seemingly Unrelated Regression through the package `systemfit`, we use the function `systemfit` with options `method=''SUR''` and `methodResidCov=''noDfCor''`.

Table 1 Time series parameter estimates for data on males and females for both The Netherlands and Belgium

	Belgium				The Netherlands			
	$\theta^{(\mathrm{BE})}$	$a^{(\mathrm{BE})}$	$\boldsymbol{V}^{(\mathrm{BE})}$		$\theta^{(\mathrm{NE})}$	$a^{(\mathrm{NE})}$	$\boldsymbol{V}^{(\mathrm{NE})}$	
Male	− 2.0372	0.9996	1.7603	− 0.1584	− 2.2333	0.9881	1.7891	0.3733
			− 0.1584	0.0649			0.3733	0.2904
Female	− 2.0029	0.8645	2.4939	− 0.0190	− 1.9368	0.9956	2.4988	− 0.2829
			− 0.0190	0.0057			− 0.2829	1.3729

European data from 1970–2009 and Dutch, Belgian data from 1970–2013, ages 0–90

country, as is visible from Table 1. This is due to the dependency between the common and country-specific time series.

Generating future scenarios of mortality For each country of interest, future mortality scenarios can be generated using the following step by step approach. We label a future scenario by $j = 1, \ldots, N$, and let t run from 2014 to some specific end year T.

1. We simulate future values of $(K_t^{(j)}, \kappa_t^{(c,j)})$ using the time dynamics specified in (19) and (20), with the parameter estimates listed in Table 1. We start with $(K_{2013}, \kappa_{2013}^{(c)})$ as obtained from the calibration strategy in Sect. 3.2. We generate i.i.d. $(\epsilon_t^{(c,j)}, \delta_t^{(c,j)})$ from a bivariate normal distribution with mean (0, 0) and covariance matrix $\boldsymbol{V}^{(c)}$ listed in Table 1.
2. From the simulated $(K_t^{(j)}, \kappa_t^{(c,j)})$ for $t = 2014, \ldots, T$, we obtain $\mu_{x,t}^{(j)}$ as in (16), (17) and (18) using the age-specific parameters $(A_x, \alpha_x^{(c)}, B_x, \beta_x^{(c)})$.

Figure 9 illustrates the projection of the time dependent parameters K_t (left) and κ_t (right) for females, Dutch (top) and Belgian (bottom) calibration. We generate 10,000 scenarios and show the corresponding fan charts (formed by the median, 0.5 and 99.5% quantiles of the generated scenarios).

Closing for old ages We use Kannistö [34] to close each mortality scenario for old ages, say $x \in \{91, 92, \ldots, 120\}$. This mortality law is chosen from a comparative analysis of techniques to close mortality tables, documented in Antonio [2]. The parametric approach of Kannistö [34] specifies the force of mortality in each scenario j, for ages $x > 90$ and a specific year t, as follows:

$$\mu_{x,t}^{(c,j)} = \frac{\phi_1^{(c,j,t)} \exp\left(\phi_2^{(c,j,t)} x\right)}{1 + \phi_1^{(c,j,t)} \exp\left(\phi_2^{(c,j,t)} x\right)}. \tag{25}$$

We estimate $(\phi_1^{(c,j,t)}, \phi_2^{(c,j,t)})$ for each scenario j and year t from the relation (as in [24])

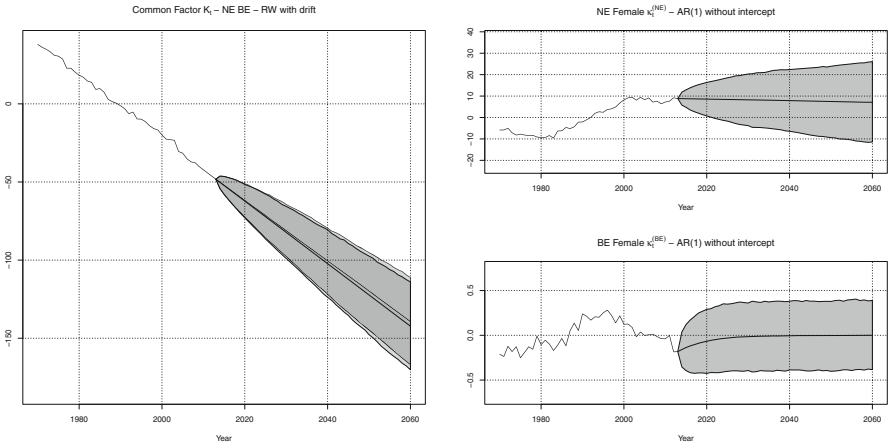

Fig. 9 Projection of time dependent parameters: K_t (left) and $\kappa_t^{(c)}$ (right) for female Dutch and Belgian data. We plot 0.5% quantile, median and 99.5% quantile obtained from 10,000 simulations. The graph on the left, with the EU trend, has two sets of quantiles due to the slightly different parameter estimation for the Dutch and Belgian data as in Table 1

$$\text{logit}\ \mu_{x,t}^{(c,j)} = \log\left(\phi_1^{(c,j,t)}\right) + \phi_2^{(c,j,t)} x, \tag{26}$$

using OLS on the ages $x \in \{80, 81, \ldots, 90\}$. The estimates for $(\phi_1^{(c,j,t)}, \phi_2^{(c,j,t)})$ are then used in (25) to determine the generated mortality scenario for ages $x > 90$.

Finally, we can switch to scenarios for future mortality rates with the transformation in (1), using

$$q_{x,t}^{(c,j)} = 1 - \exp\left(-\mu_{x,t}^{(c,j)}\right), \tag{27}$$

for $t \in \{2014, 2015, \ldots, T\}$ and $x \in \{0, 1, \ldots, 120\}$.

4 Results

4.1 Fitted and simulated mortality rates

Figure 10 shows the calibrated $\hat{q}_{x,t}^{(c)}$ for Dutch and Belgian males for a selection of ages, namely $x \in \{25, 45, 65, 85\}$. To explore the performance of the proposed model, we add extra examples with data from France and West-Germany, calibrated using the principles of Sect. 3. We show the median and 99% pointwise confidence intervals based on 10,000 scenarios of projected mortality rates. The black dots in this figure are the observed mortality rates $q_{x,t}^{(c)}$. The blue lines indicate the mortality rates fitted with the model specified in Sect. 3.1. The red lines are the calibrated mortality rates $\hat{q}_{x,t}^{(c)}$ from a country-specific Lee–Carter model. Our model is able to capture country-specific dynamics well due to the extended model specification compared to a LC model. The use of extra parameters is appropriate in view of the

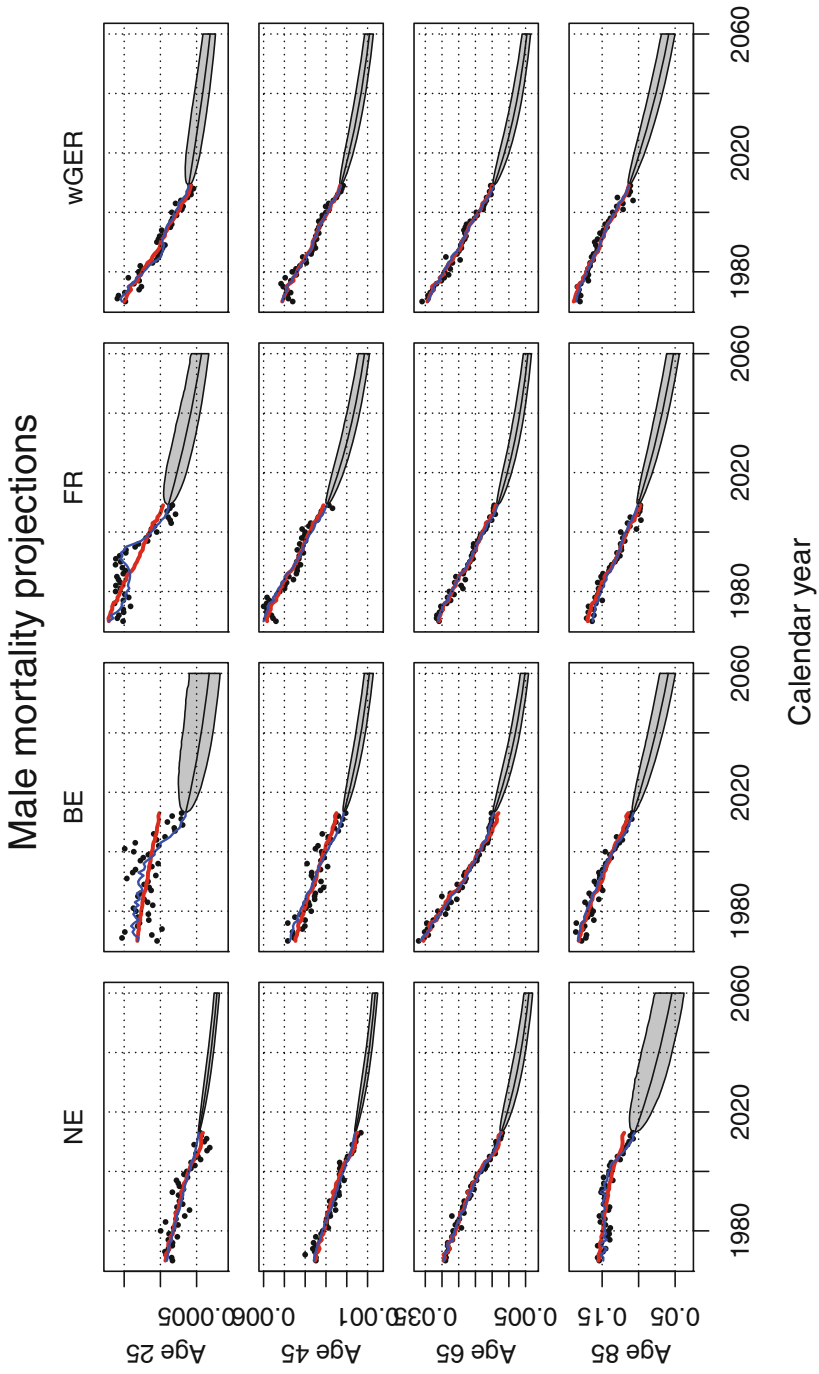
Male mortality projections
NE
BE
FR
wGER
Age 25
Age 45
Age 65
Age 85
0.0005
0.001
0.005
0.15
1980
2020
2060
Calendar year

◀**Fig. 10** Estimated (blue) and projected (grey fan chart) mortality rates, $q_{x,t}$, for The Netherlands (far left) and Belgium (middle left), male data, ages 25, 45, 65 and 85 (top to bottom). For illustration purposes, we added graphs for France (middle right) and West-Germany (far right). We plot 0.5% quantile, median and 99.5% quantile obtained from 10,000 simulations. The red line represents the single country LC calibration with the same calibration period and the black dots are the observed mortality rates

larger set of data. For example, the non-linear evolution for Dutch 85-, Belgian 25- and French 25-year old males are features which are not captured with a standard LC calibration. The French and, to a lesser extent, West-German 25-year old evolution illustrates that our model also can be a valuable improvement over the LC method for large countries with significantly larger datasets than The Netherlands or Belgium.

4.2 The best estimate tables

Based on this model, we provide point estimates of the mortality rates for all ages and years. We define the best estimate force of mortality $\hat{\mu}_{x,t}^{(c)}$ for a specific age and year as the median of the underlying distribution. These best estimates for the period effects result from (19) and (20) with noise terms $\epsilon_t^{(c)} = 0 = \delta_t^{(c)}$ for all future t. We close the mortality tables obtained in this way with Kannistö [34] such that $\hat{\mu}_{x,t}^{(c)}$ for $x \in \{0, 1, \ldots, 120\}$ and $t \in \{2014, \ldots, 2060\}$ are found. The corresponding mortality rates $\hat{q}_{x,t}^{(c)}$ follow from (1). The projected mortality tables obtained with this method result in the 'KAG 2014 projection table' and 'IA|BE 2015 mortality projection for the Belgian population'. The mortality tables are published online.[27]

4.3 Backtesting the mortality model

One of the evaluation criteria used in the process of selecting a mortality model, is its performance in backtests (see [9, 25]). We illustrate the performance of our model in two types of backtests. In the first and second row of Fig. 11 we calibrate the model on female data from 1970 to 2000 and use it to project mortality rates $q_{x,t}^{(c)}$ where $t \in \{2001, \ldots, t_{\max}\}$, with $t_{\max} = 2013$ for The Netherlands and Belgium and $t_{\max} = 2009$ for France and West-Germany. The third and fourth row of Fig. 11 visualizes the results of the backtest with calibration period 1970–2000, when the object of interest is the period life expectancy for a female aged 0 or 65. Section 5.1 gives the formal definition of the period life expectancy. The slower increase of life expectancy for The Netherlands between 1980 and 2000 has no major influence on the quality of the projections as the observed mortality rates and period life expectancies for The Netherlands are within the confidence intervals of the model.[28]

[27] For the Dutch tables, see http://www.ag-ai.nl/view.php?action=view&Pagina_Id=480. For the Belgian tables, see http://www.iabe.be/nl/iabe-mortality-tables.

[28] The Dutch calibration for this backtest initially led to an unstable AR(1) parameter in the country specific time series: $a > 1$. The results shown here are with an inequality constrained calibration for the time series to keep them stationary.

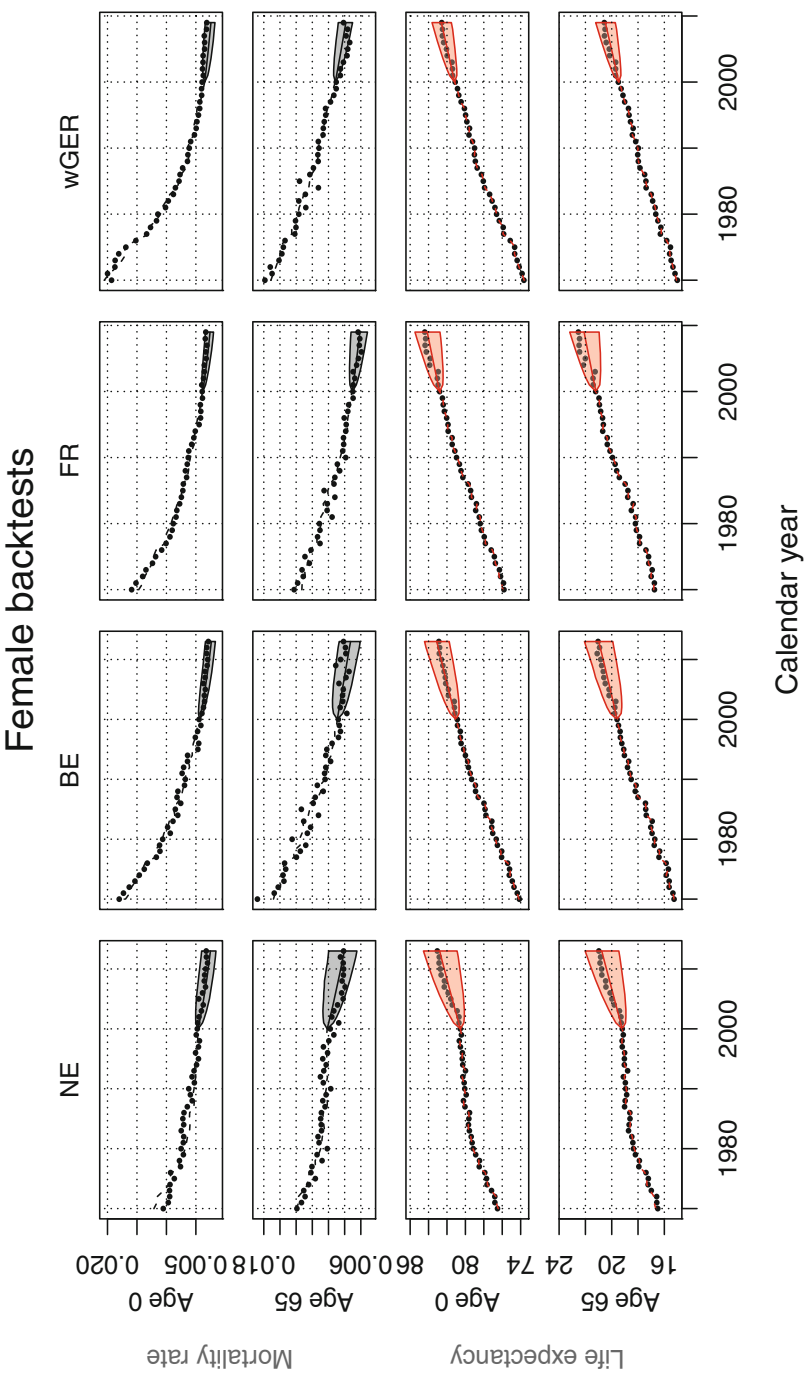
Female backtests
NE
BE
FR
wGER
Mortality rate
Life expectancy
Age 0
Age 65
Age 0
Age 65
0.020
0.005
0.018
0.006
86
80
74
24
20
16
1980
2000
1980
2000
1980
2000
Calendar year

◀**Fig. 11** Backtests with calibration period 1970–2000 for the mortality rates and period life expectancies of females aged 0 and 65, data from The Netherlands (far left) and Belgium (middle left). For illustration purposes, we added graphs for France (middle right) and West-Germany (far right). The black dots represent observed mortality rates and life expectancies, the black and red dashed lines are the calibrated rates and life expectancy and the fan charts represent the projections. We plot 0.5% quantile, median and 99.5% quantile obtained from 10,000 simulations

Overall, our model performs well in this backtest with most observations lying within the displayed quantiles for the displayed countries.

5 Applications

We discuss four possible applications of the model: the calculation and projection of life expectancies (period and cohort) to enhance insight in their future evolution, the calculation of actuarial pension corrections as suggested by the Belgian Commissie Pensioenhervorming 2020–2040 [14], the computations behind the Dutch legal retirement age updating mechanism, as well as the reserve calculations in a pension portfolio. These applications show that a carefully designed stochastic mortality model brings necessary input and tools for policy making and decision taking in the presence of life contingent risks. For all applications, our model is able to provide a (single) best estimate scenario, while—when used as a scenario generator—the model also allows to quantify uncertainty through simulations. To ease the notation, we drop the superscript (c) on the country-specific force of mortality and mortality rate.

5.1 Life expectancy: period and cohort

Using the assumption of a piecewise constant force of mortality (see (1)), the period life expectancy for an x-year old in year t is

$$e_{x,t}^{\text{per}} = \frac{1-\exp\left(-\mu_{x,t}\right)}{\mu_{x,t}} + \sum_{k\geq 1}\left(\prod_{j=0}^{k-1}\exp\left(-\mu_{x+j,t}\right)\right)\frac{1-\exp\left(-\mu_{x+k,t}\right)}{\mu_{x+k,t}}, \tag{28}$$

and the cohort life expectancy for an x-year old in year t is

$$e_{x,t}^{\text{coh}} = \frac{1-\exp\left(-\mu_{x,t}\right)}{\mu_{x,t}} + \sum_{k\geq 1}\left(\prod_{j=0}^{k-1}\exp\left(-\mu_{x+j,t+j}\right)\right)\frac{1-\exp\left(-\mu_{x+k,t+k}\right)}{\mu_{x+k,t+k}}, \tag{29}$$

see, for example, Pitacco et al. [43].[29] The period definition only uses the forces of mortality of one specific year t. As such, when mortality data is available for that particular year, the corresponding period life expectancy can immediately be calculated using (28). In contrast, the cohort definition uses forces of mortality from not only year t but also the future years. To obtain numerical results for (29)

[29] We note that the KAG uses a slightly different definition of life expectancies, available on page 34 of Koninklijk Actuarieel Genootschap [37].

Fig. 12 Period (black dots and red lines) and cohort (blue) life expectancy for a 0-year old (row 1 and 3) ▶ and 65-year old (row 2 and 4) for The Netherlands (far left) and Belgium (middle left), female (top rows) and male (bottom rows) data. For illustration purposes, we added graphs for France (middle right) and West-Germany (far right). We plot 0.5% quantile, median and 99.5% quantile obtained from 10,000 simulations

mortality data and forecasts are necessary for several subsequent years. Since a person experiences mortality rates over successive years, the cohort life expectancy is a more appropriate concept when quantifying the amount of years an individual is expected to live. We therefore encourage the use of the cohort definition when addressing life expectancy. From the mortality scenarios generated as described in Sect. 3.3 we obtain simulations of the period and cohort expectancy, $e_{x,t}^{\text{per}}$ and $e_{x,t}^{\text{coh}}$. When calculating cohort life expectancies in, say, 2060, we need to project the mortality rates over a horizon of 120 years beyond 2060. Next to the paths generated for the period and cohort life expectancy, the best estimate table, introduced in Sect. 4.2, generates a point estimate of these quantities.

Figure 12 shows the observed period life expectancy (black dots) for a 0 and a 65-year old Dutch, Belgian, French and West-German female and male, the calibrated period life expectancy (red line) and confidence intervals of the projected period and cohort life expectancies: $e_{0,t}^{\text{per}}$, $e_{65,t}^{\text{per}}$, $e_{0,t}^{\text{coh}}$ and $e_{65,t}^{\text{coh}}$ for $t \in \{2014, \ldots, 2060\}$. The model captures the observed, in-sample period life expectancies for different countries very well.

Tables 2 and 3 list the 0.5, 50 and 99.5% quantiles of $e_{x,t}^{\text{coh}}$ for specific choices of x and t for the Dutch and Belgian calibration. Dutch males have higher best estimate cohort life expectancy than their Belgian counterparts whereas for females the differences are in favour of the Belgians, though considerably smaller. The Dutch projections have significantly wider confidence intervals because the variance of the country-specific time series κ_t is larger for The Netherlands than for Belgium for both genders, as the covariance matrix in Table 1 underpins.

5.2 Pension cost and actuarial corrections

Pension liabilities are increasing because of decreasing mortality rates and hence increasing life expectancies. It is imperative to use scenarios generated by a carefully designed mortality model to obtain sound forecasts of the evolution of pension liabilities. These forecasts bring insight in the consequences of retirement at a specific age and allow institutions to take appropriate measures to keep pension costs sustainable. For some illustrations in this section, we use period life expectancy instead of its cohort counterpart because it is known for past years and relies on a smaller projection horizon for future years. Therefore uncertainty is smaller for the period than for the cohort life expectancy.

The model presented in this paper can readily be used to picture the evolution of pension costs. We hereby assume constant interest rates in order to remove the interest rate risk and to focus exclusively on longevity risk. Let us consider an x-

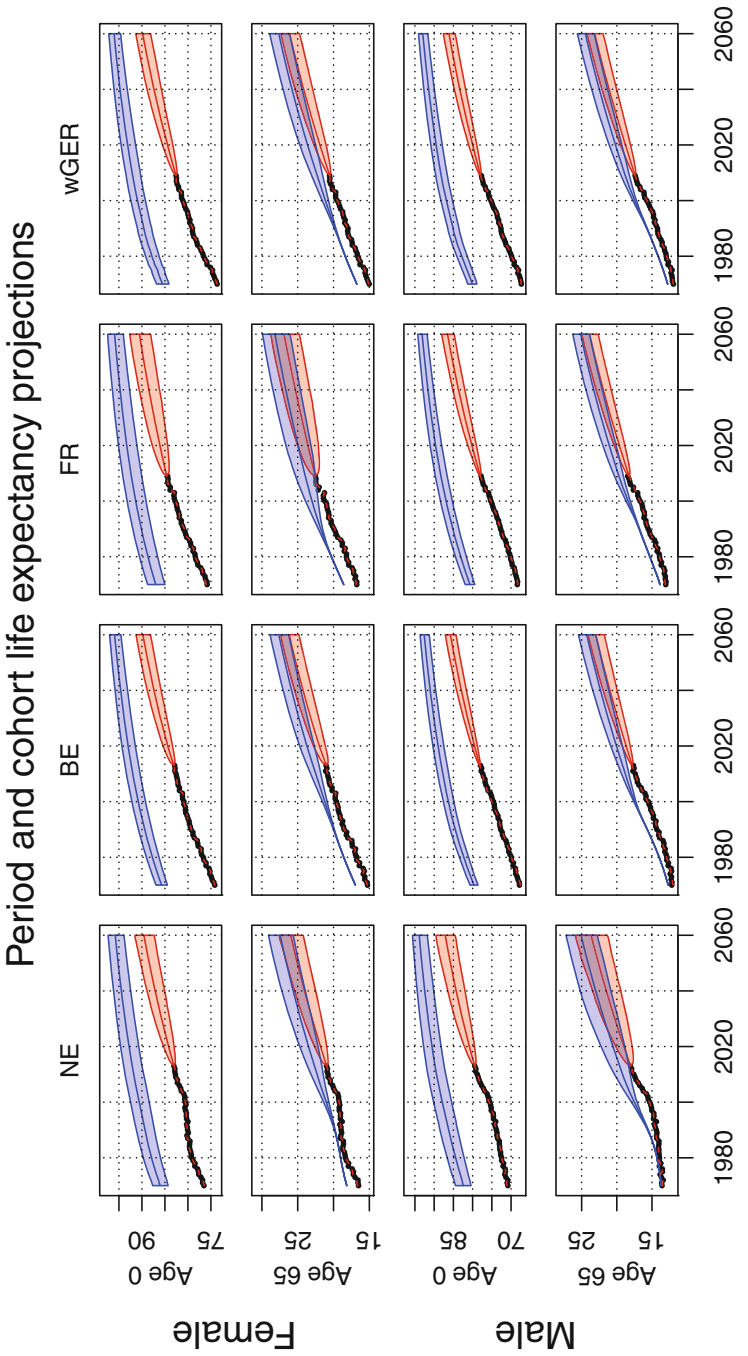
Period and cohort life expectancy projections
NE
BE
FR
wGER
Female
Male
Age 0
Age 65
Calendar year
1980
2020
2060

Table 2 Cohort life expectancy for a Dutch 0- and 65-year old, best estimate and 0.5, 50 and 99.5% quantiles obtained from 10,000 simulations, for males and females

The Netherlands		Males		Females	
Year		0 [0.5%; 50%; 99.5%]	65 [0.5%; 50%; 99.5%]	0 [0.5%; 50%; 99.5%]	65 [0.5%; 50%; 99.5%]
2014	Best estimate	89.89	19.74	92.22	22.78
		[87.42; 89.89; 92.03]	[18.36; 19.74; 21.11]	[90.07; 92.22; 94.11]	[21.71; 22.78; 23.83]
2040	Best estimate	92.45	23.02	94.51	25.64
		[90.18; 92.44; 94.42]	[20.76; 23.02; 25.10]	[92.45; 94.51; 96.23]	[23.91; 25.65; 27.24]
2060	Best estimate	93.87	25.08	95.82	27.46
		[91.84; 93.87; 95.65]	[22.72; 25.08; 27.25]	[93.91; 95.82; 97.40]	[25.69; 27.46; 29.12]

Table 3 Cohort life expectancy for a Belgian 0- and 65-year old, best estimate and 0.5, 50 and 99.5% quantiles obtained from 10,000 simulations, for males and females

Belgium		Males		Females	
Year		0 [0.5%; 50%; 99.5%]	65 [0.5%; 50%; 99.5%]	0 [0.5%; 50%; 99.5%]	65 [0.5%; 50%; 99.5%]
2014	Best estimate	88.26	19.30	92.40	22.98
		[86.74; 88.26; 89.48]	[18.63; 19.31; 19.96]	[90.80; 92.39; 93.81]	[22.09; 22.98; 23.82]
2040	Best estimate	91.04	22.33	94.66	25.85
		[89.61; 91.03; 92.19]	[21.15; 22.33; 23.40]	[93.16; 94.65; 95.93]	[24.56; 25.84; 27.03]
2060	Best estimate	92.61	24.28	95.95	27.64
		[91.31; 92.60; 93.62]	[22.96; 24.28; 25.38]	[94.60; 95.95; 97.08]	[26.23; 27.64; 28.85]

year old Belgian pensioner in year t who receives a yearly pension of €10,000. The present value of the cash flow which represents his yearly future pension allowance is expressed as follows, see Dickson et al. [23]:

$$\mathrm{PV}_{x,t}(10{,}000) = 10{,}000 \cdot \ddot{a}_{x,t} \tag{30}$$

$$= 10{,}000 \cdot \sum_{k \geq 1} \left(\frac{1+g}{1+i}\right)^{k} \prod_{l=0}^{k-1} (1 - q_{x+l,t+l}), \tag{31}$$

where g is the inflation or indexation factor, i is the interest rate and $(1 - q_{x+l,t+l})$ is the one-year survival probability of an $x + l$-year old in year $t + l$. Using (31) and the mortality projections from our model, we obtain the evolution of the pension cost $\mathrm{PV}_{65,t}(10{,}000)$ of a 65-year old Belgian over time, visualized by the blue band in Fig. 13 (left).[30] We see a fast increase of the pension cost $\mathrm{PV}_{65,t}(10{,}000)$ over the years as the life expectancy increases. To design sustainable pension systems in an era of increasing expenses, governments are currently implementing different types of measures, as mentioned in Sect. 1. An increase of the legal pension age, like in Belgium, linking the legal pension age to the evolution of the life expectancy and adjustments to the benefits, as in The Netherlands, are typical examples of such measures. As a first illustration of the measures suggested by the Belgian 'Commissie Pensioenhervorming 2020–2040', we show how to develop career sensitive actuarial corrections which adjust the pension costs for people who retire earlier or later than the '*normal pension age*'. The latter is the age at which one reaches a '*full career*', for example, after having worked for 45 years.[31] To calculate fair corrections we take the ratio of (31) for two different ages and years. We consider the situation where the full career of an individual corresponds to retirement at the normal pension age x_n in year t_n, whereas his actual situation corresponds to retirement age x_r reached in year t_r. For this specific individual we then have $t_n = t_r + (x_n - x_r)$. With the inflation rate g equal to the interest rate i we represent a situation with constant purchasing power, which leads to the following equation:

$$\frac{\mathrm{PV}_{x_n,t_n}(10{,}000)}{\mathrm{PV}_{x_r,t_r}(10{,}000)} = \frac{\sum_{k \geq 1} \prod_{l=0}^{k-1} (1 - q_{x_n+l,t_n+l})}{\sum_{k \geq 1} \prod_{l=0}^{k-1} (1 - q_{x_r+l,t_r+l})}. \tag{32}$$

The two quantities on the right hand side of (32) are closely related to the cohort life expectancies from (29).[32] As such, in case of early retirement, $x_r < x_n$ and the numerator of (32) is smaller than the denominator. Hence, the ratio becomes smaller than 1, indicating increasing pension costs due to retiring before the normal pension age. For $x_r > x_n$ the reverse conclusions apply.

[30] The interest rate i is set to a constant 1% and inflation g is ignored, i.e. 0%. The red band in the left panel of Fig. 13 are period calculations of $\mathrm{PV}_{65,t}(10{,}000)$, obtained by replacing $q_{x+l,t+l}$ in (31) with $q_{x+l,t}$.

[31] The age at which one reaches a full career, i.e. the normal pension age, can be different from person to person depending, amongst others, on the age one starts working and any period of inactivity on the way.

[32] The quantities are actually '*curtate*' cohort life expectancies, see, for example, Dickson et al. [23].

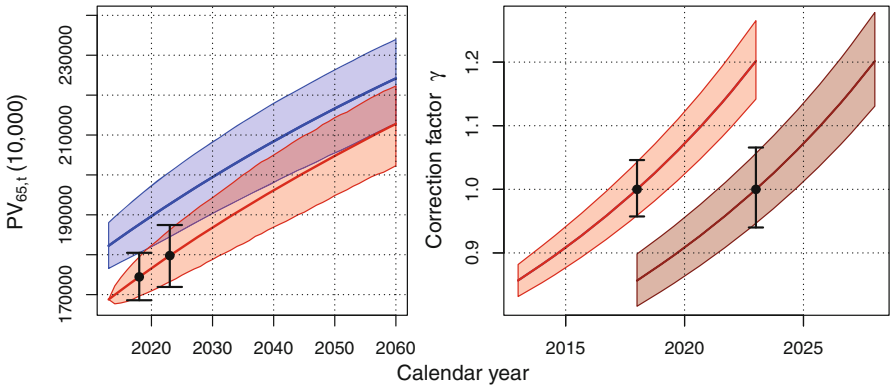

Fig. 13 Left: evolution from 2013 to 2060 of the pension cost of a 65-year old Belgian with a yearly pension of €10,000, no inflation applied and a constant interest rate of 1%. The blue band represent cohort calculations as in (31) and the red band represent period calculations using mortality rates from one year at a time. Right: Actuarial corrections over time on pension benefits for two cohorts of people: with normal pension age 65 in year 2018 (light red) and with normal pension age 65 in year 2023 (dark red). All simulations of the period life expectancy of a 65-year old retiring in 2018 and 2023 respectively were taken as a reference point and combined with all other simulations. Reference points are denoted by • and **I** in both panels. We plot 0.5% quantile, median and 99.5% quantile obtained from 10,000 simulations

In order to compensate the increased pension cost due to early retirement, the Belgian 'Commissie Pensioenhervorming 2020–2040' suggests to apply an actuarial correction γ in the following way:

$$B_{x_r,t_r} = 10{,}000 \cdot \gamma = 10{,}000 \cdot \tau \cdot \frac{e_{x_n,t_n}}{e_{x_r,t_r}}, \tag{33}$$

where B_{x_r,t_r} is the adjusted benefit corresponding to retirement at age x_r in year t_r, where 10,000—in our example—is the benefit one would receive in case of retirement without any correction,[33] $e_{x,t}$ is the period life expectancy at age x in year t and τ is a factor determining the strength of the actuarial correction with $\tau = 1$ leading to a full correction. In this example we will assume $\tau = 1$. The period life expectancy is used here to calculate the right hand side of (33) since this demographic marker is observable (every year) and its forecasts do not rely on a long forecasting horizon. The ratio of period life expectancies $e_{x,t}$ in (33) serves the same purpose as the ratio in (32). As such, with the adjusted benefit B_{x_r,t_r} obtained from (33), the actuarial present value of his future benefits $\mathrm{PV}_{x_r,t_r}(B_{x_r,t_r})$ is equal to the actuarial present value of his benefits $\mathrm{PV}_{x_n,t_n}(10{,}000)$, in case of retirement at the normal pension age. This correction will financially penalize people who retire before the normal pension age, because their higher life expectancy will lead to reduced benefits, and reward people who work longer than the normal pension age while keeping a fair balance in the total costs for one person. The Belgian

[33] This is the benefit one would receive in case of retiring at normal pension age x_n in year t_n but calculated using the individual's situation regarding pension variables (such as career length, social security status,...) at age x_r in year t_r. Thus, only the timing/mortality aspect of benefits is taken into account.

'Commissie Pensioenhervorming 2020–2040' suggests to calculate the normal pension age x_n and the subsequent actuarial corrections γ on an individual basis.[34] Consider two individuals, one aged 60 in 2013 and the other aged 60 in 2018 with normal pension age $x_n = 65$ in year $t_n = 2018$ respectively 2023. With the period life expectancy of a 65-year old in 2018 respectively 2023 as reference point (i.e. $e^{\text{per}}_{65,2018}$ and $e^{\text{per}}_{65,2023}$), we calculate the actuarial corrections γ in the right graph of Fig. 13, similar to the procedure in Devolder and Maréchal [22] (see Tableau 3), but making use of the simulations of our model. If the person, aged 60 in 2013, retires in 2013, he will receive only 84–89% of his yearly unadjusted benefit whereas if he decides to delay his pension to the age of 70 in 2023 he will receive 114–126% of the yearly unadjusted benefit. The uncertainty is due to the uncertainty in the reference point $e^{\text{per}}_{65,2018}$ and the uncertainty in period life expectancies in years 2014–2023.[35] For 60-year olds in 2018, similar conclusions can be drawn for the correction factors, showing that this calculation of correction factors ensures solidarity within individual cohorts of people with the same birth year and normal pension age, but not between different cohorts.

In the previous illustration, all people retiring at the normal pension age will receive full benefits. Hence, pension costs continue to increase due to an increasing life expectancy, as shown in Fig. 13 (left). The actuarial corrections γ can also be applied to keep pension costs more stable over time, with respect to the pension cost for a pensioner who retires at age x_n in a fixed reference year t_n. That is the point of view developed in our second illustration. By fixing the reference year t_n for the whole population, irrespective of year of birth or when one reaches the normal pension age x_n, the correction factor in (33) will ensure that the total pension cost for an individual aged x_r in year t_r is fixed at $\text{PV}_{x_n,t_n}(B_{x_r,t_r})$ for all x_r and t_r.[36] We calculate the correction factors γ in (33) for people retiring at age 60 (black), 65 (red), 67 (blue) and 70 (orange) in future years with the reference life expectancy e_{x_n,t_n} fixed at the observed period life expectancy for age $x_n = 65$ in year $t_n = 2013$. Figure 14 (left) shows the evolution of pension costs over time for different ages if no actuarial correction is applied. The case of a 65-year old (red band) is the same as for the period calculations in Fig. 13 (left). We calculate the actuarial corrections with the period life expectancy of a 65-year old in 2013 as reference point in Fig. 14 (right). An early retirement at the age of 60 before 2020 will decrease the pension benefits by almost 20% and more in later years. In contrast, retirement at the age of 70 in 2013 gives a 25% increase in pension benefits, but retiring at the age of 70 in 2060 will probably lead to a decrease in pension benefits driven by increasing life

[34] As such, it is possible that one person has a normal pension age of 67 while another has a normal pension age of 62, depending on career length, type of profession, etc. See Commissie Pensioenhervorming 2020–2040 [14] for more information.

[35] Since there are 10,000 simulations for the reference point and 10,000 simulations for all period life expectancies from 2014 onwards, the quantiles were calculated on $10{,}000 \times 10{,}000$ evaluations of the correction factor γ. For the year 2013, only 10,000 evaluations were necessary since $e^{\text{per}}_{60,2013}$ is known and observed.

[36] Of course, the benefit B_{x_r,t_r} is still dependent on the situation of the underlying individual, but the numerator numerator of the actuarial correction γ in (33) is now the same for the whole population.

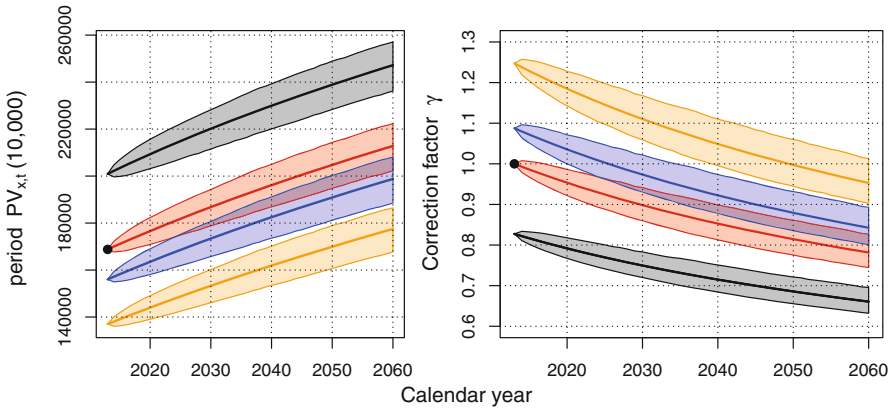

Fig. 14 Left: period calculations of the evolution from 2013 to 2060 of the pension cost of a 60 (black), 65 (red), 67 (blue) and 70 (orange) year old Belgian with a yearly pension of €10,000, no inflation applied and a constant interest rate of 1%. Right: actuarial corrections on pensions for retiring at the age of 60 (black), 65 (red), 67 (blue) and 70 (orange) with the scenario of a 65-year old retiring in 2013 as a reference point, denoted by • in both panels. We plot 0.5% quantile, median and 99.5% quantile obtained from 10,000 simulations

expectancy, all relative to the reference point of the period life expectancy of a 65 years old in year 2013.

The 'Commissie Pensioenhervorming 2020–2040' also stresses that socially motivated adjustments to this system will be necessary because life expectancy is not homogeneous over the whole population. For example, blue-collar workers like construction workers tend to have a significantly lower life expectancy than white-collar workers. With proper data the methods laid out in this paper are readily extendable to profession specific mortality calculations. Villegas and Haberman [51] use related models to quantify the mortality differences in the UK between subpopulations with different socio-economic backgrounds.

5.3 Evolution of the Dutch retirement age

As discussed in Sect. 1, the legal retirement age in The Netherlands is linked to the evolution of the period life expectancy (PLE) of a 65-year old via the AOW-law.[37] In this section we use our model to project the Dutch legal retirement age in accordance with the current Dutch law. The model allows us to capture both the best estimate evolution and the uncertainty of projections of the legal retirement age. De Waegenaere et al. [20] present an initial discussion of this policy using the LC model, and Stevens [49] compares different retirement age policies, based on the LC and Cairns et al. [8] model.

Starting from 2013, the legal retirement age in The Netherlands will increase from the age of 65 to the age of 67 in 2021. This increase is deterministic and Fig. 15 (see years 2013–2021 in the graphs) illustrates the specific legal retirement

[37] This section is based on the Dutch retirement law (AOW-law) as consulted on 29 April 2016: http://wetten.overheid.nl/BWBR0002221/.

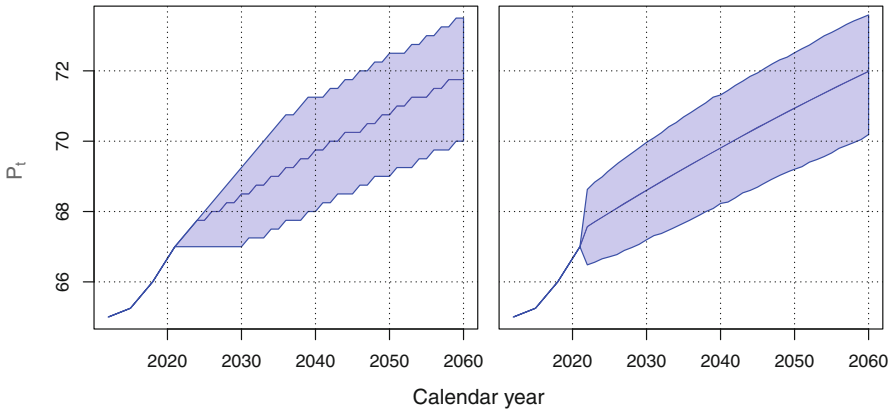

Fig. 15 Left: simulated evolution of retirement age P_t according to our model, using the formulas and restrictions of the AOW-law (34–36). Right: simulated evolution of retirement age P_t according to our model, using the formulas of the AOW-law, but without restrictions on the maximum or minimum yearly increase (not taking into account (36)). We plot 0.5% quantile, median and 99.5% quantile obtained from 10,000 simulations

age P_t for every year t, set by the Dutch legislators. From 2022 onwards, the retirement age P_t for year t is linked to the PLE as follows:

$$P_t = P_{t-1} + V_t \quad \text{with } P_{2021} = 67 \tag{34}$$

$$V'_t = (e^{\text{per}}_{65,t} - 18.26) - (P_{t-1} - 65) \tag{35}$$

$$V_t = 0 \cdot I(V'_t < 0.25) + 0.25 \cdot I(V'_t \geq 0.25), \tag{36}$$

where $I(\cdot)$ is the indicator function, $e^{\text{per}}_{65,t}$ refers to the PLE of a 65-year old in year t as in (28). V'_t captures the increase in PLE with respect to the average PLE of a 65-year old in 2000–2009, that is $e^{\text{per}}_{65,2000:2009} = 18.26$. This way, if $e^{\text{per}}_{65,t} > 18.26$ in a future year t and this is not compensated by a similarly higher retirement age P_{t-1} (from the previous year) compared to $P_{2000:2009} = 65$, (35) will be positive and lead to an increased retirement age P_t according to (34). Equation (36) limits the increase in pension age such that either no increase or an increase of three months occurs. We refer to this as the restricted increase. When the yearly increase V_t in (34) is calculated using V'_t instead of V_t, we refer to it as the unrestricted increase.

The reference point $e^{\text{per}}_{65,2000:2009} = 18.26$ in the mechanism presented in (34)–(36) was determined by CBS. The CBS is in charge of the calculation of the legal retirement age and has to determine the retirement age P_t five years up front. For example, on 1 January 2017, CBS will estimate $e^{\text{per}}_{65,2022}$ and together with $P_{2021} = 67$ and (34)–(36), this leads to the retirement age P_{2022}. This illustrates the necessity for a careful projection methodology, as presented in this paper.

Using the formulas for $e^{\text{per}}_{x,t}$ from (28) and our mortality scenario generator we calculate the restricted and unrestricted yearly increases V_t and V'_t and subsequently the future retirement age P_t for 10,000 simulations. For this

application, the model was calibrated on the aggregated female and male datasets to obtain a unisex approach.[38] The retirement age P_t in the restricted case, as in the AOW-law, is plotted in the left panel of Fig. 15. The median retirement age over all scenarios predicts subsequent three month increases in the legal retirement age P_t from 2022 to 2024 because the period life expectancy for a 65-year old in 2022 ($e^{\text{per}}_{65,2022}$) and beyond is significantly higher than 20.26 in most simulations.[39] A retirement age of $P_t = 68$ is reached in 2026 with the median scenario. The right panel of Fig. 15 shows the retirement age P_t in the unrestricted case. An immediate, relatively large increase is observed in 2022 which is in accordance with the restricted case where multiple sequential increases are necessary to accommodate this first jump in the unrestricted case. After the first jump, the retirement age increases at a steady rate.

5.4 Cashflow projections for stylized portfolios

It is imperative for insurance companies and pension funds to accurately predict their future liabilities and to hedge these liabilities with sufficient assets. To illustrate the impact of the mortality scenarios from our model on books with life contingent liabilities, we determine the future cashflows of six stylized portfolios. The strategy outlined below can be used by pension funds or insurance companies to evaluate the impact of future mortality scenarios on their liabilities. The portfolios under consideration, taken from Koninklijk Actuarieel Genootschap [37], hold three types of liabilities summarized below.

- Lifelong pension benefits or main benefits (MB). These are yearly benefits, payable from retirement on until the passing of the insured.
- Latent lifelong partner benefits (lPB). These are yearly benefits, payable to the partner of the insured upon the death of the insured, regardless of the age of the insured or the partner. The payments stop when the partner dies. Both the insured and partner are still alive at the starting point so no payments have been incurred yet.
- Lifelong partner benefits already incurred (iPB). Similar to the latent partner benefits but the payments have already started due to the death of the insured.

Koninklijk Actuarieel Genootschap [37] gives the composition of the portfolios and distinguishes a young, middle aged and old portfolio, per gender.[40] Figure 16 visualizes the number of insureds (further denoted as '*exposure*') in the different portfolios per age class and per type of benefit. The young portfolios have more exposure in the younger age classes and less exposure in the older age classes when

[38] This approach is slightly different from the unisex methodology of CBS.

[39] The value 20.26 is obtained by filling in $P_{2021} = 67$ in (35) and simplifying, leading to $e^{\text{per}}_{65,2022}$ being compared with $18.26 + 2$. If the predicted PLE is significantly higher than this number (e.g. 8 months higher), subsequent yearly three month increases are necessary to compensate for this difference.

[40] See Appendix B of the English version of the KAG publication: http://www.ag-ai.nl/view.php?action=view&Pagina_Id=625.

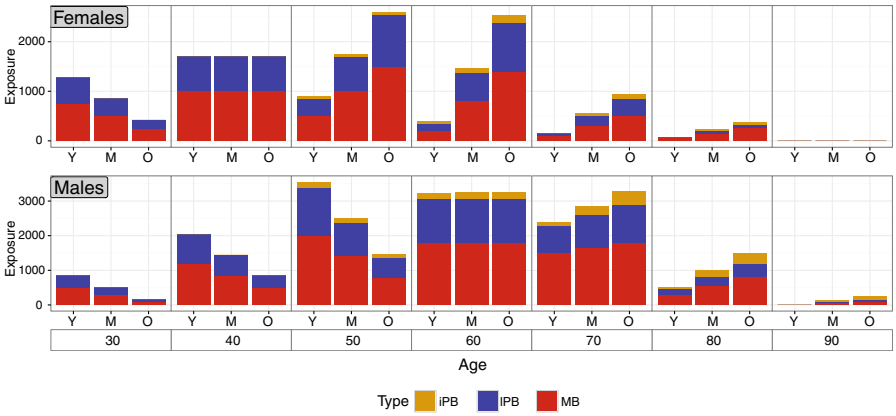

Fig. 16 Exposures per age class and per benefit type for the young (Y), middle aged (M), and old (O) portfolios. Male portfolios (top) and female portfolios (bottom)

Table 4 Assumptions made on the portfolio calculations of Sect. 5.4

#	Assumption
1	The retirement age x_r is fixed at 65
2	Nobody becomes older than 121
3	We assume a 100% partner frequency of opposite gender. Partner benefits for the male portfolios are therefore paid to their female partners and vice versa
4	In each couple, the male is always 3 years older than the female
5	No lapses
6	The liability is 1 per head and paid at 1 January every year
7	The starting date is 1 January 2014
8	We assume realistic interest rates provided by the Dutch National Bank

compared to the old portfolios. The middle aged portfolio exposures are in between the other ones.

We generate scenarios of future cashflows for these portfolios via the simulations for future mortality rates as discussed in Sect. 3.3. To ease the portfolio calculations, we use a set of assumptions listed in Table 4.

Denote with $\mathcal{C} = \{1, \ldots, 7\}$ the different age classes of the portfolio and for each class $c \in \mathcal{C}$, $x_c \in \{30, 40, \ldots, 90\}$ is the age of the people in class c which is rounded down to the decade.[41] $\mathrm{E}_{c,l}$ is the exposure of liability $l \in \{\mathsf{MB}, \mathsf{IPB}, \mathsf{iPB}\}$ in class c. Using this notation, the present value (in year 2014) of a cashflow in year $2014 + t$ per type of liability in a specific male portfolio, is calculated as follows (see [23]):

[41] For example, all people in the portfolio aged 40-49 are in class $c = 2$ and have their age rounded to $x_c = 40$. This is assumed because we do not have full portfolio data but only exposures per age class.

$$\mathsf{MB}_t = \sum_{c\in\mathcal{C}} I(x_c + t \geq 65) \cdot \mathrm{E}_{c,\mathsf{MB}} \cdot {}_tp^{\mathrm{M}}_{x_c,2014} \cdot \left(\frac{1}{1+i_t}\right)^t; \tag{37}$$

$$\mathsf{IPB}_t = \sum_{c\in\mathcal{C}} \mathrm{E}_{c,\mathsf{IPB}} \cdot {}_tp^{\mathrm{F}}_{x_c-3,2014} \cdot (1 - {}_tp^{\mathrm{M}}_{x_c,2014}) \cdot \left(\frac{1}{1+i_t}\right)^t; \tag{38}$$

$$\mathsf{iPB}_t = \sum_{c\in\mathcal{C}} \mathrm{E}_{c,\mathsf{iPB}} \cdot {}_tp^{\mathrm{F}}_{x_c-3,2014} \cdot \left(\frac{1}{1+i_t}\right)^t; \tag{39}$$

with $I(\cdot)$ the indicator function and i_t the interest rate at time $2014 + t$ using the interest rate curve of 31 May 2014 published by the Dutch National Bank.[42] ${}_tp^{\mathrm{G}}_{x,2014}$ is the probability that an x-year old in 2014 of gender 'G' will live for another t years, which follows from the mortality rates of Sect. 3.3:

$${}_tp_{x,2014} = \prod_{l=0}^{t-1} (1 - q_{x+l,2014+l}). \tag{40}$$

To obtain (37)–(39) for the female portfolios, the genders F and M have to be switched and the male partner is considered to be three years older than the female partner. Every simulation of future mortality rates leads to a scenario of survival probabilities ${}_tp_{x,2014}$ and subsequently to one expected cashflow scenario. We do not consider interest rate risk so the interest rate curve is the same for all scenarios. This way, the uncertainty reported in the following graphs and table is only due to uncertainty in future mortality.

Figure 17 shows the present values of the cashflows of the male portfolios for the main benefits MB_t, the summed partner benefits $\mathsf{IPB}_t + \mathsf{iPB}_t$ and the total benefits. The first row shows the undiscounted expected cashflows (with $i_t = 0$ in (37)–(39)) and the second row contains the same cashflows discounted to 1 January 2014. The upward jumps occur when a new age class reaches the retirement age every 10 years. They are an artefact of the composition of our portfolios, where ages are rounded down to the decade. The old portfolios reach their peak expected cashflows earlier than the young portfolios because more insureds are already retired or close to retirement at the start of the calculations. Over time the expected cashflows from the middle and young portfolio overtake the old portfolio's expected cashflows. Since partner benefits are paid regardless of the age of the partner, these graphs show a more continuous evolution over time. The total expected cashflow is obtained by summing (37), (38) and (39) over time. This cashflow for a specific portfolio is the present value of all future payments (PVFP). If no premiums are earned, it is the capital the fund should hold in order to cover its future liabilities, if the assumptions in the technical basis are met. Figure 18 (right) gives statistics on the simulated PVFP of the *middle aged male portfolio* relative to its best estimate, i.e. the PVFP calculated with the best estimate table from Sect. 4.2. The 99.5% quantile of the PVFP is 2.6% larger than the best estimate PVFP. Figure 18 (left)

[42] As in Table 1.3.1 on http://www.dnb.nl/statistiek/statistieken-dnb/financiele-markten/rentes/index.jsp.

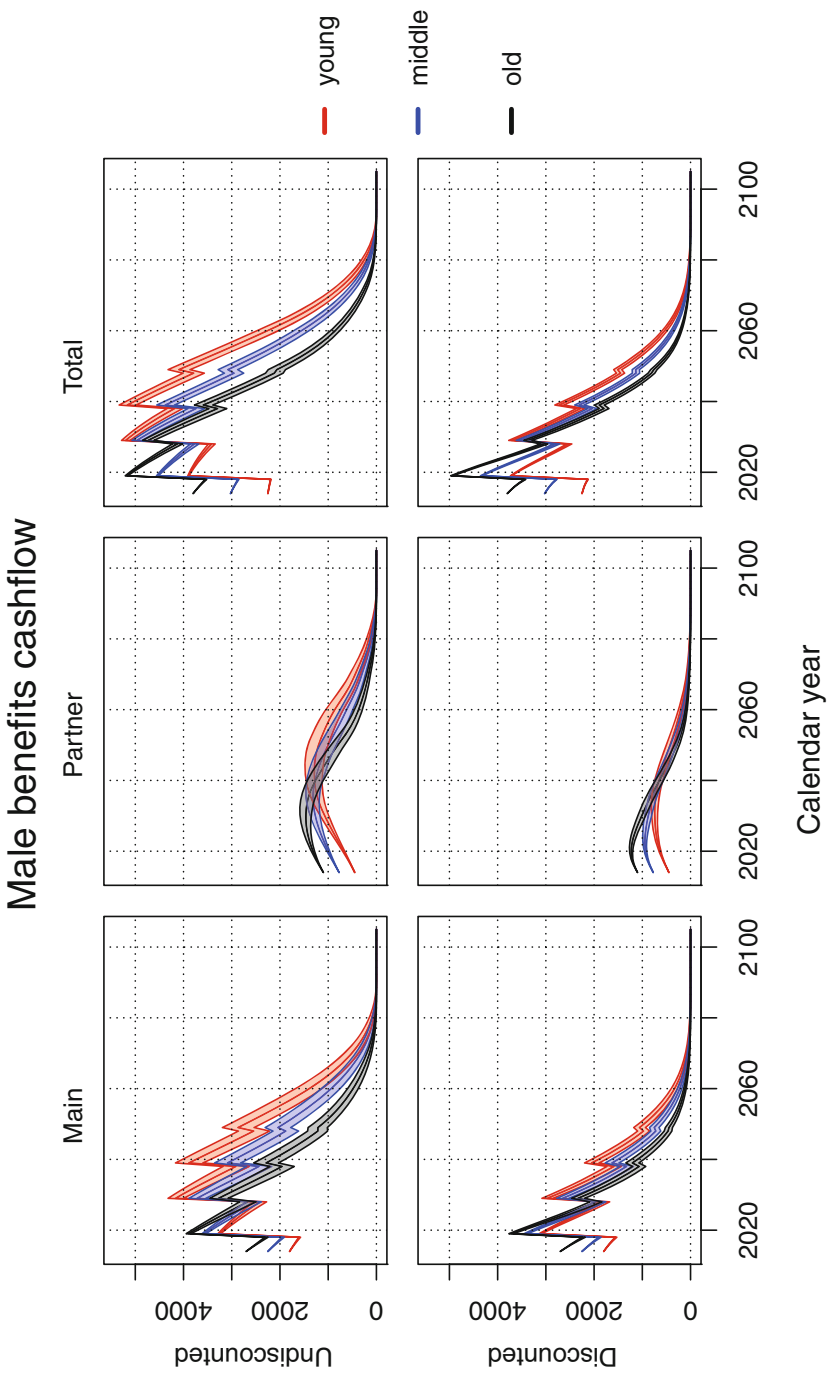
Male benefits cashflow
Main
Partner
Total
young
middle
old
Undiscounted
Discounted
0
2000
4000
2020
2060
2100
Calendar year

◀**Fig. 17** Portfolio cashflows over time for the benefits of the 3 male portfolios. The young portfolio cashflow is in red, the middle in blue and the old in grey. The first row contains the undiscounted cashflows and the second row represents the cashflows discounted to 1 January 2014. We plot 0.5% quantile, median and 99.5% quantile obtained from 10,000 simulations

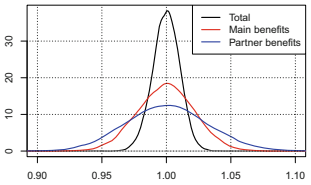

	MB	PB	Total
Best Est.	74,422	31,214	105,636
mean	74,392 (99.96%)	31,230 (100.05%)	105,622 (99.99%)
sd	1,627 (2.2%)	989 (3.2%)	1,094 (1.0%)
75%	75,491 (101.5%)	31,892 (102.2%)	106,371 (100.7%)
95%	77,074 (103.6%)	32,866 (105.3%)	107,377 (101.6%)
99.5%	78,499 (105.5%)	33,820 (108.3%)	108,385 (102.6%)

Fig. 18 Left: kernel density estimates of the middle male portfolio PVFP relative to the best estimate PVFP. Total portfolio PVFP (black), main benefit PVFP (red) and partner benefit PVFP (blue) based on 10,000 simulations. Right: Absolute values of the best estimate PVFP (first row) and basic statistics and quantiles of the 10,000 simulated PVFP of the middle male portfolio. Percentages indicate the value relative to the best estimate PVFP. PB refers to the sum of both the latent and the already incurred partner benefits

shows kernel density estimates of the PVFP of the middle male portfolio for the different liabilities, relative to the best estimate PVFP. It is important for insurance companies and pension funds to quantify the impact of a range of plausible mortality scenarios through an appropriate stochastic mortality model in order to take well informed risk management decisions. After all, the capital buffer a company should hold is greatly affected by the calculation of the PVFP. Additionally, new data has to be incorporated every year to evaluate the impact on the capital buffers.

6 Conclusions

This article documents the process of creating an industry wide standard for mortality projections in The Netherlands and Belgium, an assignment given to the joint team of authors of this paper by the Dutch (in 2014) and Belgian (2015) professional actuarial bodies. The resulting stochastic mortality model is a multi-population model of Li and Lee type on the complete age range which combines an overall European trend with a country specific deviation from this trend. Apart from explaining historical mortality data, the model acts as a generator of scenarios for future mortality. The paper illustrates four possible applications of such scenarios; the calculation and projection of demographic indicators (e.g. life expectancy) with focus on their future evolution, the calculation of actuarial pension corrections correcting for early or late retirement, the computations in a legal retirement age updating mechanism that is linked to evolutions in life expectancy, and the calculation of liabilities in a pension portfolio. These applications readily demonstrate the potential impact of our work on life contingent calculations in society.

Our contributions are threefold. First, we carefully explain how mortality statistics collected from different sources, each with its own pace of refreshing and

own data reporting standards, can be combined using concepts from Lexis diagrams. Second, using a set of criteria inspired by academic literature as well as practical concerns, we motivate why we opt for the Li and Lee model. We highlight the in- and out-of-sample performance of this model, the plausibility of the scenarios it generates and its status as a consensus between academic and practical insights. We carefully document the many model choices made during the development process: the set of countries used in the multi-population setting, the calibration and projection methodology, and the technique to close the resulting mortality rates for old ages.

The evaluation of the performance of the mortality model when new data becomes available is imperative, and should be done on a regular basis. As topics for future research we identify the need for statistical tools that assist the modeller in the choice of countries to be included in the multi-population setting, and the development of a Bayesian calibration strategy to allow for a joint calibration and projection approach taking all sources of uncertainty into account. To ensure coherent forecasts, a new estimation strategy for the time series can be developed by choosing an appropriate prior for the time series parameters in a Bayesian estimation setting or by applying an iterated constrained generalized least squares algorithm in the Seemingly Unrelated Regression approach. We encourage a further stimulation by actuarial institutions of blended research teams, where academics and practitioners construct 'best practices', meeting rigorous scientific standards as well as practical usefulness.

Acknowledgements The authors would like to thank the two anonymous referees who provided helpful suggestions to improve an earlier draft of this paper. The authors acknowledge the support of the *Koninklijk Actuarieel Genootschap* and the *Institute of Actuaries in Belgium*. Katrien and Sander are grateful for the financial support of *Ageas Continental Europe*, *Fonds voor Wetenschappelijk Onderzoek* (FWO) and the support from KU Leuven through the C2 COMPACT research project.

References

1. Albrecher H, Embrechts P, Filipović D, Harrison G, Koch P, Loisel S, Vanini P, Wagner J (2016) Old-age provision: past, present, future. Eur Actuar J 6(2):287–306
2. Antonio K (2012) Sluiten van de periodetafel GBM/V 2005–2010. http://www.ag-ai.nl
3. Antonio K, Devolder L, Devriendt S (2015) The IA|BE 2015 mortality projection for the Belgian population. https://lirias.kuleuven.be/bitstream/123456789/487077/1/AFI_15101.pdf
4. Barrieu P, Bensusan H, El Karoui N, Hillairet C, Loisel S, Ravanelli C, Salhi Y (2012) Understanding, modelling and managing longevity risk: key numbers and main challenges. Scand Actuar J 3:203–231
5. Börger M, Fleischer D, Kuksin N (2014) Modeling the mortality trend under modern solvency regimes. ASTIN Bull 44(1):1–38
6. Brouhns N, Denuit M, Vermunt J (2002) A Poisson log-bilinear regression approach to the construction of projected life tables. Insur Math Econ 31:373–393
7. Cairns A (2007) LifeMetrics open source R code. http://www.macs.hw.ac.uk/~andrewc/lifemetrics/. JPMorgan Chase Bank
8. Cairns A, Blake D, Dowd K (2006) A two-factor model for stochastic mortality with parameter uncertainty: theory and calibration. J Risk Insur 73:687–718
9. Cairns A, Blake D, Dowd K, Coughlan G, Epstein D, Ong A, Balevich I (2009) A quantitative comparison of stochastic mortality models using data from England and Wales and the United States. N Am Actuar J 13(1):1–35

10. Cairns A, Blake D, Dowd K, Kessler A (2016) Phantoms never die: living with unreliable population data. J R Stat Soc Ser A (Stat Soc) 179(4):975–1005
11. Cairns A, El Boukfaoui G (2017) Basis risk in index based longevity hedges: a guide for longevity hedgers. Working Paper, Heriot-Watt University, Edinburgh. http://www.macs.hw.ac.uk/∼andrewc/papers/HedgingLongevityRisk2017.pdf
12. Carter L, Lee R (1992) Forecasting demographic components: modeling and forecasting US sex differentials in mortality. Int J Forecast 8:393–411
13. Chen H, MacMinn R, Sun T (2015) Multi-population mortality models: a factor copula approach. Insur Math Econ 63:135–146
14. Commissie Pensioenhervorming 2020–2040 (2014). Een sterk en betrouwbaar sociaal contract. Voorstellen van de Commissie Pensioenhervorming 2020–2040 voor een structurele hervorming van de pensioenstelsels. http://www.pensioen2040.belgie.be
15. Commissie Pensioenhervorming 2020–2040 (2015) Zware beroepen, deeltijds pensioen en eerlijke flexibiliteit in het pensioensysteem. Aanvullend advies van de Commissie Pensioenhervorming 2020–2040. http://www.pensioen2040.belgie.be
16. Czado C, Gneiting T, Held L (2009) Predictive model assessment for count data. Biometrics 65(4):1254–1261
17. D'Amato V, Haberman S, Piscopo G, Russolillo M, Trapani L (2014) Detecting common longevity trends by a multiple population approach. N Am Actuar J 18(1):139–149
18. D'Amato V, Haberman S, Piscopo G, Russolillo M, Trapani L (2016) Multiple mortality modeling in a Poisson Lee–Carter framework. Commun Stat Theory Methods 45(6):1723–1732
19. Dawid A, Sebastiani P (1999) Coherent dispersion criteria for optimal experimental design. Ann Stat 27:65–81
20. De Waegenaere A, Melenberg B, Boonen T (2012) Het koppelen van de pensioenleeftijd en pensioenaanspraken aan de levensverwachting. Netspar Design Papers, 12
21. Denuit M, Goderniaux A-C (2005) Closing and projecting life tables using log-linear models. Bull Swiss Assoc Actuar 1:29–48
22. Devolder P, Maréchal X (2007) Réforme du régime belge de pension légale basée sur la longévité. Belg Actuar Bull 7:34–38
23. Dickson D, Hardy M, Waters H (2009) Actuarial mathematics for life contingent risks. Cambridge University Press, Cambridge
24. Doray L (2008) Inference for the logistic-type models for the force of mortality. In: Living to 100 and beyond, SOA Monograph M-LI08-01, pp 1–18
25. Dowd K, Cairns A, Blake D, Coughlan G, Epstein D, Khalaf-Allah M (2010) Backtesting stochastic mortality models. N Am Actuar J 14(3):281–298
26. Enchev V, Kleinow T, Cairns A (2017) Multi-population mortality models: fitting, forecasting and comparisons. Scand Actuar J 2017(4):319–342
27. European Commission (DG ECFIN) and Economic Policy Committee (Ageing Working Group) (2015) The 2015 ageing report: Economic and budgetary projections for the 28 EU member states (2013–2060). Eur Econ 3. http://ec.europa.eu/economy_finance/publications/european_economy/2015/pdf/ee3_en.pdf
28. Haberman S, Kaishev V, Millossovich P, Villegas A, Baxter S, Gaches A, Gunnlaugson S, Sison M (2014) Longevity basis risk: a methodology for assessing basis risk. Technical report, Institute and Faculty of Actuaries. https://www.actuaries.org.uk/documents/longevity-basis-risk-methodology-assessing-basis-risk
29. Haberman S, Renshaw A (2011) A comparative study of parametric mortality models. Insur Math Econ 48:35–55
30. Hyndman R, Booth H, Yasmeen F (2013) Coherent mortality forecasting: the product-ratio method with functional time series models. Demography 50(1):261–283
31. IMF (2012) Global financial stability report—the quest for lasting stability. http://www.imf.org/External/Pubs/FT/GFSR/2012/01/pdf/text.pdf
32. Institute and Faculty of Actuaries (2012) CMI Working paper 63. http://www.actuaries.org.uk/research-and-resources/pages/cmi-working-paper-63
33. Institute of Actuaries and Faculty of Actuaries (1973) Continuous mortality investigation reports. http://www.actuaries.org.uk/research-and-resources/documents/cmi-report-1-whole-volume
34. Kannistö V (1992) Development of the oldest-old mortality, 1950–1990: evidence from 28 developed countries. Odense University Press, Odense

35. Kleinow T (2015) A common age effect model for the mortality of multiple populations. Insur Math Econ 63:147–152
36. Koninklijk Actuarieel Genootschap (2012) Prognosetafel AG2012. http://www.ag-ai.nl/view.php?action=view&Pagina_Id=496
37. Koninklijk Actuarieel Genootschap (2014) Prognosetafel AG2014. http://www.ag-ai.nl/view.php?action=view&Pagina_Id=535
38. Lee R, Carter L (1992) Modeling and forecasting the time series of US mortality. J Am Stat Assoc 87:659–671
39. Li J (2013) A Poisson common factor model for projecting mortality and life expectancy jointly for females and males. Popul Stud J Demogr 67(1):111–126
40. Li N, Lee R (2005) Coherent mortality forecasts for a group of populations: an extension of the Lee–Carter method. Demography 42(3):575–594
41. National Association of Insurance Commissioners (2013) NAIC model rule (regulation) for recognizing a new annuity mortality table for use in determining reserve liabilities for annuities. http://www.naic.org/store/free/MDL-821.pdf. MDL-821
42. Niu G, Melenberg B (2014) Trends in mortality decrease and economic growth. Demography 51(5):1755–1773
43. Pitacco E, Denuit M, Haberman S, Olivieri A (2009) Modeling longevity dynamics for pensions and annuity business. Oxford University Press, Oxford
44. Plat R (2009) On stochastic mortality models. Insur Math Econ 45:393–404
45. Renshaw A, Haberman S (2006) A cohort-based extension to the Lee–Carter model for mortality reduction factors. Insur Math Econ 38:556–570
46. Schwarz G (1978) Estimating the dimension of a model. Ann Stat 6(2):461–464
47. Shang H (2016) Mortality and life expectancy forecasting for a group of populations in developed countries: a multilevel functional data method. Ann Appl Stat 10(3):1639–1672
48. Society of Actuaries (2014) Mortality improvement scale MP-2014. http://www.soa.org/Research/Experience-Study/Pension/research-2014-mp.aspx
49. Stevens R (2016) Managing longevity risk by implementing sustainable full retirement age policies. J Risk Insur. doi:10.1111/jori.12153
50. Van Berkum F, Antonio K, Vellekoop M (2016) The impact of multiple structural changes on mortality predictions. Scand Actuar J 2016(7):581–603
51. Villegas A, Haberman S (2014) On the modeling and forecasting of socioeconomic mortality differentials: an application to deprivation and mortality in England. N Am Actuar J 18(1):168–193